JMEPEG (2021) 30:3003–3023
https://doi.org/10.1007/s11665-021-05584-9


1059-9495/$19.00

# Influence of Processing Parameters on Surface Properties of SKD61 Steel Processed by Powder Mixed Electrical Discharge Machining

*Van Tao Le*

Submitted: 2 December 2020 / Revised: 16 January 2021 / Accepted: 11 February 2021 / Published online: 4 March 2021

**Many studies have carried out on the characteristics of surfaces processed by PMEDM with various powders. However, limited works have used the tungsten carbide powder in the PMEDM process and investigated its effects on the surface properties. In this research, the influence of main process parameters, including the peak current ($I_p$), the pulse on time ($T_{on}$), and the powder concentration ($C_p$) on surface properties—i.e., surface roughness ($R_a$), microhardness of surfaces (HV), and surface morphology of SKD61 steel machined by PMEDM with tungsten carbide powder, was explored in two modes: the fine-finish mode and the semi-finish mode. The results show that the peak current, the pulse on time, and the powder concentration have a noticeable influence on surface properties. The surface roughness, the microhardness of surfaces, and the surface morphology at the small peak current ($I_p$ =1 A) and the short pulse on time ($T_{on}$ =16 µs) were improved better than those at the large peak current ($I_p$=4 A) and the long pulse on time ($T_{on}$ =200 µs) with all powder concentrations. The best improvement of the surface roughness at $I_p$=1 A; $T_{on}$=16 µs; $C_p$=40 g/l is 0.471 ± 0.011µm with a reduction of 57.984% as compared to the normal EDM. The set of processing parameters {$I_p$=1 A; $T_{on}$=16 µs; $C_p$=60 g/l} has the most positive effect on the improvement of microhardness and surface morphology: The microhardness was enhanced up to 825 ± 19 HV with an increase of 129.167% as compared to the normal EDM. The surface morphology had the smooth surface, the few micro-cracks, the few voids, the few droplets, and the few globules of debris as compared to that of other process parameters and the normal EDM.**

**Keywords** EDM, microhardness, powder, surface morphology, surface roughness

## 1. Introduction

Electrical discharge machining (EDM) is largely used to process metals with high hardness and/or metals that are difficult to be cut, for example SKH54, Ti6Al4V alloy, SKD61. However, the EDM process generally features a low removing rate of material and a low surface quality. To enhance the productivity and the quality of machined surfaces in EDM, the conductive powder is generally mixed into the dielectric liquid of the EDM process. Such a EDM process is also named the powder mixed electrical discharge machining (PMEDM) process. PMEDM has improved the spark discharge process. The participation of conductive powder in spark discharge process enables reducing the electrical insulation ability of the dielectric fluid, varied the electrical discharge gap between the tool and the workpiece (Ref 1-3). In high-temperature conditions, free electrons in the conductive particle of powder have reduced the insulation of the dielectric fluid. The improvement of electrical conductivity in the dielectric fluid has assisted sparks to be formed from a further distance and thus has widened the discharge distance (Ref 4-6). In addition, the electrical sparks are more uniform, and the discharge channel is widely extended. The spark discharge is reduced in energy, and the craters become shallower (Ref 7-9). Therefore, the process of spark discharge becomes stable, enhances the machining performance and the surface quality (Ref 10-13).

The first research on the PMEDM process was reported in 1980 (Ref 14), which reported on the influence of Al, Fe, and C powder mixed into the dielectric liquid of the EDM process on the surface quality and the machinability of samples. After that, a series of studies have been reported. The authors studied a

**Van Tao Le**, ATC, Le Quy Don Technical University, Hanoi, Viet Nam. Contact e-mail: taoitd@yahoo.com.

**List of symbols**

| | |
|---|---|
| $I_p$ | Peak current (A) |
| $T_{on}$ | Pulse on time (µs) |
| $T_{off}$ | Pulse off time (µs) |
| $C_p$ | Concentration of powder (g/l |

**Abbreviations**

| | |
|---|---|
| EDM | Electrical discharge machining |
| PMEDM | Powder mixed electrical discharge machining |
| MRR | Material removal rate |
| EWR | Electrode wear ratio |
| TWR | Tool wear rate |
| MDR | Material deposition rate |
| RLT | Recast layer thickness |
| EDX | Energy-dispersive x-ray spectroscopy |
| SEM | Scanning Electron Microscope |

wide variety of powders. In addition, assistance measures (Ref 10, 13, 15, 16) including the vibration of tool and/or workpiece electrode, and assistance of electromagnetic fields in the PMEDM process have been performed. For example, Nguyen et al. (Ref 17) reported the change in the surface properties of samples by the EDM process with Ti. The authors demonstrated that the surface roughness was decreased, and the microhardness of surfaces was significantly increased as compared to the EDM process. Marashi et al. (Ref 18) investigated the effect of $TiO_2$ powder in the EDM process on surface properties of AISI D2 steel. As a result, the craters were shallower. Microdefects were reduced on the surface of workpieces. Chen and Lin (Ref 19) investigated the combination of TC powder and ultrasonic tool in the EDM process to process Al-Zn-Mg material. The results show that the EDM process with the TC powder and ultrasonic tool has improved the surface roughness, the microhardness, the material removal rate (MRR), and the electrode wear ratio (EWR) as compared to that of the normal EDM.

In (Ref 20), the authors used chromium powder in the EDM process and assessed the influence of such a powder on MRR, tool wear rate (TWR), EWR, and surface roughness of H11 steel. The Taguchi method was applied to optimize the goals including the MRR, the TWR, the EWR, and the surface roughness. The result had found the positive process parameter for improvement of the machining ability and the surface roughness. Microhardness, micro-cracks, and surface morphology of H11 steel were studied (Ref 21) with the participation of Cr particles in the EDM process. The results have shown that the microhardness, the micro-cracks, and surface morphology were improved as compared to that of the EDM process.

Prakash et al. (Ref 22) studied the change in the surface properties of titanium alloy-Ti35Nb7Ta5Zrβ by the EDM process with Si powder. The authors have reported a significant improvement in surface modification, MRR, and TWR. The surface properties of Ti6Al4V steel were investigated by Li et al. (Ref 23) when SiC powder was added into the insulating oil of the EDM process with the assistance of magnetic stirring. The results showed that the surface properties including surface topography and microhardness were improved. The surface properties and machinability of Inconel 718 Alloy were investigated by Kumar Sahu et al. (Ref 24) when SiC powder was added to the dielectric liquid of the EDM process. The authors pointed out that the addition of powder improved significantly surface roughness, MRR, and surface structure as compared to the normal EDM process. AISI D2 steel were studied by Al-Khazraji et al. (Ref 25) on surface modification in EDM process with the addition SiC powder. Two types of tool electrode have been used including copper and graphite electrode. The results showed that the thickness of the white layer, the fatigue life, and microhardness of surfaces have significantly improved as compared to the EDM method. Authors also pointed out the suitability of each type tool electrode with added powder for surface modification. The SiC powder was added to the dielectric liquid of the EDM process. It was reported by Öpöz et al. (Ref 26). The surface modification of Ti6Al4V steel by this PMEDM process has been investigated. The results showed that the microhardness increased due to SiC penetration into the surface of samples.

Some other powders including Al, Mo, reduced graphene oxide, carbon nanotubes, $CeO_2$, and $MoS_2$ have also been studied, specifically as follows: Rouniyar et al. (Ref 27) investigated the influence of Al powder on the surface properties of aluminum 6061 alloy by the EDM process with the aid of a magnetic field. The results showed that the surface roughness, recast layer thickness, and surface morphology was improved as compared to normal EDM. Amorim et al. (Ref 28) investigated surface modification of H13 steel with the addition of Mo powder after the machined EDM process. The research results showed that molybdenum powder in the EDM process had great domination on the properties of recast layers. And the size of molybdenum powder had also great domination on the properties of recast layers. The addition of the reduced graphene oxide powder in the EDM process was studied by Świercz et al. (Ref 29). In this research, the authors have reported a change in surface properties of 55NiCrMoV7 steel. The roughness of surfaces and the thickness of recast layers had a significant decrease as compared to the EDM process. In addition, there is an assessment of the white layer thickness formation with positive polarity and negative polarity. Carbon nanotubes (CNTs) powder has been added into the dielectric fluid to process Ti6Al4V alloy by the EDM process, which was reported by Shabgard et al. (Ref 30). Authors have shown that MRR, TWR, surface quality including surface roughness, and micro-cracks have been significantly improved. Hossain et al. (Ref 31) reported that the influence of $CeO_2$ powder, with particle size is less than 5 mm, mixed in the pure water. Results for MRR, TWR, surface roughness, microhardness, and micro-crack have been improved as compared to conventional EDM with different concentrations. At concentration of 0.6 g/l MRR, TWR, surface roughness, microhardness, and micro-crack have achieved the most optimal value. A combination of suspended $MoS_2$ powder with ultrasonic frequency vibration has been experimented with by Prihandana et al. (Ref 32). The experimental results were reported that the MRR and the surface quality were improved after machining.

In addition, several studies have used different powders in the same study to evaluate the role of each powder for surface modification in the EDM process. For example, Talla et al. (Ref 5) studied the influence of three types of powder including Al, Gr, and silicon powder in the EDM process on Inconel 625. The authors point to the effect of each type of powder to improve the surface quality and the MRR. Gr powder had the biggest influence on the improvement of MRR. But the silicon powder had the biggest influence on the improvement of surface microhardness. Jabbaripour et al. (Ref 33) studied Al, Gr, SiC, Cr, and Fe powders in the EDM process to improve the surface roughness of TiAl material. The results showed that the biggest improved surface roughness of the EDM process with Al powder reduced by 32% as compared to the normal EDM process. The surface of samples by the machined PMEDM is more resistant to corrosion than those by the machined normal EDM.

Recently, very few studies focused on the effect of tungsten powder on the surface modification of workpieces by the EDM process. Kumar and Batra (Ref 34) studied the effect of the addition tungsten powder into the dielectric fluid on the microhardness of surfaces of three type of OHNS, D2, and H13 steel. The authors stated that the microhardness of surfaces of three types of steel was increased by more than 100%, leading to increase the wear resistance of the machined surface. This improvement in the surface's wear resistance is very valuable for the mold and die, as well as components that require a high abrasion resistance. Bhattacharya et al. (Ref 35) investigated the effect of the tungsten powder adding to the dielectric liquid to process the copper material with a W-Cu electrode that gave

a fine surface after work, showing specifically that the microhardness of surfaces was significantly improved. Mohanty et al. (Ref 36), Ti6Al4V steel investigated for surface modification during EDM machining with the participation of tungsten disulfide ($WS_2$) powder mixed in deionized water. The results showed a significant improvement in the microhardness (HV), the recast layer thickness (RLT), the material deposition rate (MDR), and the surface roughness. In their study, the wear resistance tests were also performed. The results showed a better wear resistance of PMEDM surface than that of normal EDM.

As mentioned above, many researchers employed different powders in the EDM process to achieve desired surface qualities for specific applications. However, limited studies have reported on the effect of tungsten carbide powder on the surface modification of SKD61 steel processed by PMEDM. Tungsten Carbide is a metallic element with a high melting temperature (about 3422°C), a low thermal expansion, and high strengths. Its resistance to oxidation, acid, and alkali corrosion is also very good. SKD61 steel is largely in the hot stamping, tool, die, and machine parts. SKD61 steel is a material with good mechanical properties, especially when it is chemically or heat-treatment. Thus, this study aims to analyze, evaluate the influence trend of main process parameters including peak current ($I_p$), pulse on time ($T_{on}$), and powder concentration ($C_p$) on the surface properties (including the surface roughness, the microhardness of surfaces, and the surface morphology) of SKD61 steel in the EDM process with tungsten carbide powder at fine-finish and semi-finish modes.

## 2. Materials and Methods

Figure 1 shows the experimental diagram of this study, which is composed of three blocks. The first block presents the input parameters, including system and process parameters. The next block represents the PMEDM process. The final block shows the output parameters. The surface roughness, microhardness of surfaces, and surface morphology are analyzed and evaluated in different scenarios of using the main process parameters.

### 2.1 Materials

In the experiment, SKD61 steel supplied by Daido corporation of Japan was used. Its chemical composition is composed of 0.38%C-1%Si-5%Cr-1.25%Mo-1%V-0.4%Mn. The oil EDM fluid 2 was used as a dielectric fluid. It was supplied by the manufacturer Shell. The tungsten carbide powder with code WC-727-6 used in this experiment was supplied by the manufacturer Praxair Surface Technologies. Its chemical composition consists of 5.56%C-11.9%Co-0.02%Fe-82.5%W-0.02% of other components. The particle diameter is less than 31 μm.

### 2.2 Methods

Samples were machined on the electrical discharge machine from Aristech Company with model CNC-460 EDM (Fig. 2). The dimensions before and after machining were given in Table 1. Before the samples and copper electrodes were put into machining by PMEDM process. They were machined with high accuracy in terms of geometric dimensions (0.01 mm) and geometric errors (0.02 mm) by the fine grinding method, then the samples and tool electrodes were attached to the CNC-460 EDM, which was carefully mounted with high precision. The purpose of this has made the PMEDM process to be the most accurate. The powder was added to the dielectric fluid in the tank. It has dimensions of length × width × height = 320 × 250 × 220 mm. It was contained 14 liters of the dielectric fluid. The powder concentration was determined before the machining and mid machining process. The purpose of this is to determine the powder concentration and maintain the powder concentration. Principle of determination of the powder concentration: Use a graduated flask containing the mixture of oil and powder, which was taken out of the tank. When the powder in the graduated flask was settled completely to the bottom of the flask. The powder and oil were separated, the weight of the powder and the volume of the oil were determined, which leads to the determination of the powder concentration.

Criteria and basis for selection of process parameters: For electrical parameters, based on the literature overview and the configuration of the controller settings of the electrical discharge machine—the CNC-460 EDM. In addition, the aim of this study was to evaluate the surface properties in the fine-finish and semi-finish modes. Among electrical parameters, peak current and pulse on time had a strong impact on the surface properties of SKD61 steel (Ref 36-39). Hence, the main domination of electrical parameters including the peak current, and the pulse on time was selected. Variable levels of these electrical parameters were chosen as shown in Table 1. Other parameters such as the discharge voltage, the pulse off time, and polarity of the electrode were fixed as shown in Table 1. For powder concentration, it was through the exploratory tests on the basis of the electrical parameters selected as above, combined with the thermal and electrical properties of the tungsten carbide powder. Hence, variable levels of powder concentration in this experiment were selected as shown in Table 1.

Surface roughness of the samples ($R_a$) was carried out the surface roughness tester with model TR200, it was supplied from TINE Group. The surface roughness tester was set up with a cutoff length of 0.8mm, and a track length of 4mm. Value of surface roughness in each technology mode was the average value of the three different measurement areas on machined surface of the sample. These average values of surface roughness were analyzed and evaluated in the following section.

Content of the tungsten element was measured by energy-dispersive x-ray spectroscopy (EDX) method on the JSM6610LA-Jeol machine. It was the average value of measurement result on three different measurement regions of the sample, obtained after the machined process. It was set up as shown in Fig. 3. The content of the tungsten element in this study was used for analysis and evaluation in the following section. Surface morphology of machined samples was taken by Scanning Electron Microscope (SEM) on the JSM6610LA-Jeol machine. The images of surface morphology were used to analyze and evaluate in the following section.

The microhardness of surfaces was performed on microhardness tester Duramin-Struers. A load of 980.7 mN was applied for more over 10 s. The microhardness in each technology mode was the average value of the three different measurement points on the cross-sectional of the machined surface layer. The average microhardness of surfaces was analyzed and evaluated in the following section.

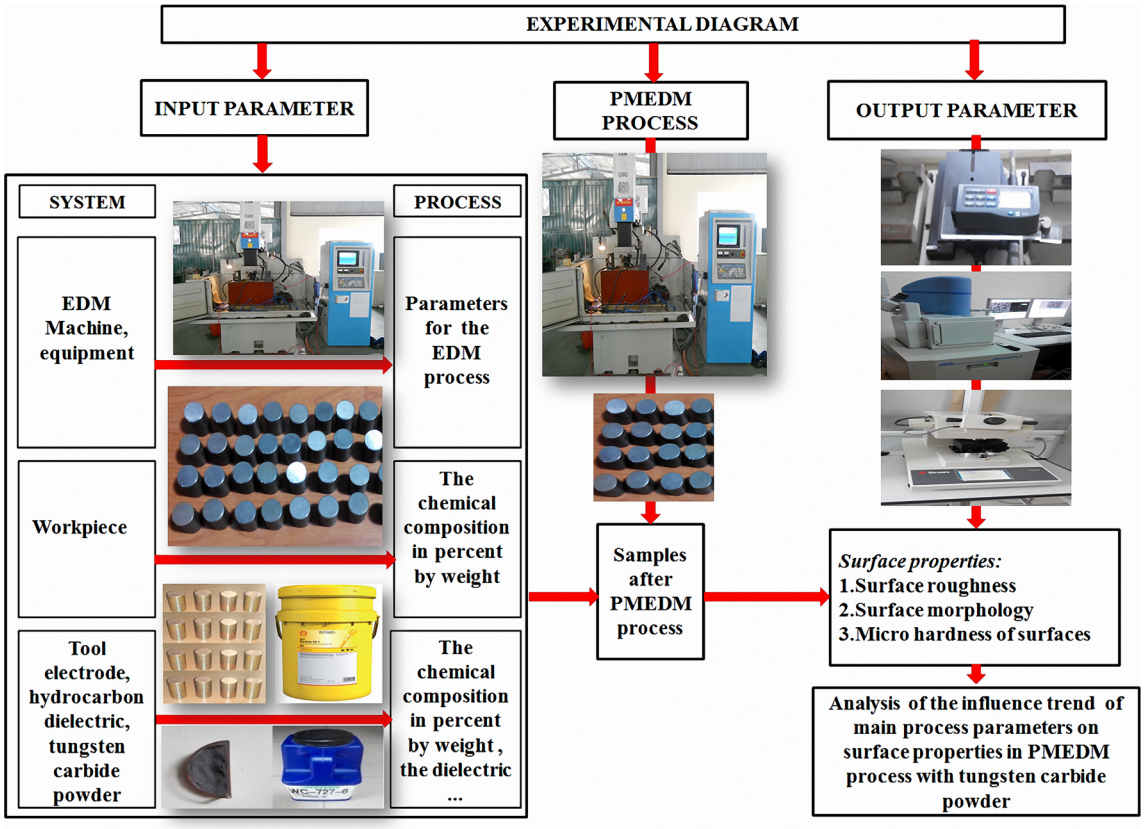


**Fig. 1** Experimental diagram of study

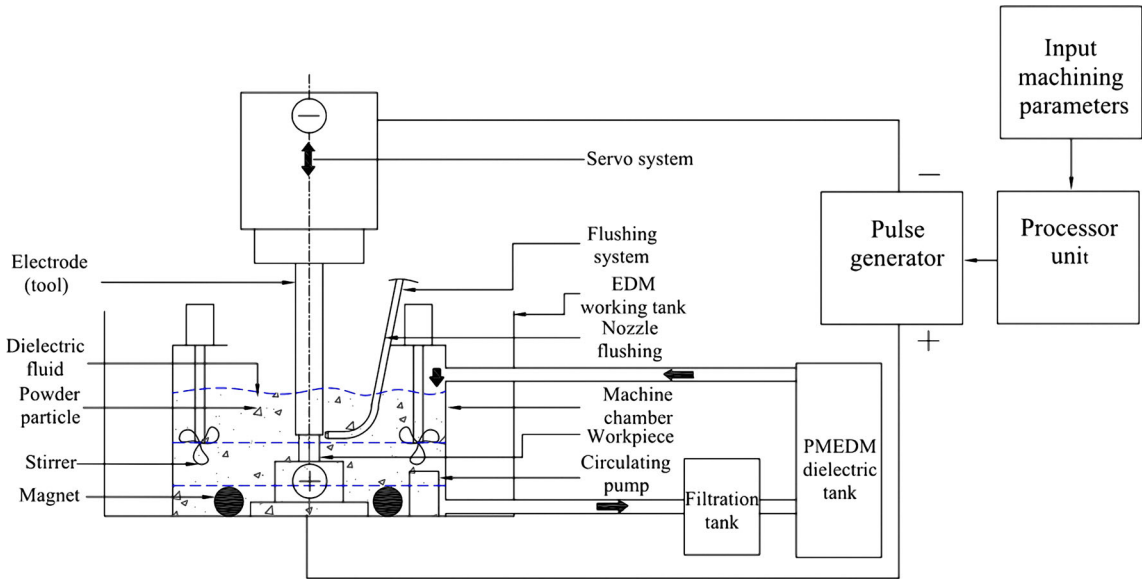


**Fig. 2** Principle schema of the PMEDM system

X-ray diffraction (model: X'Pert PRO, make: PANalytical, from Netherlands) was performed to determine the organization of the tungsten carbide phase on the machined surface as in Fig. 4. The x-ray data were analyzed using X'Pert High Score plus software to identify the tungsten carbide phase. The diffraction angle ($2\theta$) was taken in the range of $0^{\circ}$ and $90^{\circ}$. The presence of the tungsten carbide phase has been detected, such as $W_2C$, $WC_{1-x}$.

## 3. Results and Discussion

### 3.1 Surface Roughness ($R_a$)

The surface roughness was observed from Fig. 5 and 6. The surface roughness by the PMEDM process is improved better than the EDM process in all of the pulse on time and all of the peak current. The surface roughness varies with the direction of

**Table 1 Experimental conditions**

| Deposition condition | Detail |
|---|---|
| Peak current, A $I_p$ | 1 A; 4 A |
| Pulse on time, μs $T_{on}$ | 16 μs; 200 μs |
| Pulse off time, μs $T_{off}$ | 50 μs |
| The dielectric fluid | Shell EDM Fluid 2 |
| Polarity of electrode | Negative (−) |
| Tool electrode | Cu (99%) |
| Current voltage, V | 120 V |
| Concentration of powder, g/l $C_p$ | 20;40;60 |
| Dimension of sample | D × L= 19× 50 mm |
| Dimension after machining | D× L=19× 49.7 mm |

reduction. This can be illustrated by the participation of conductive powder in the discharge process. However, the surface roughness change is more or less. This depends on the combination of electrical parameters and powder concentration. This is the cause, many or few conductive powder particles have been involved in the spark discharge process, changed the spark discharge process in the following respects:

a. The conductive powder is mixed into the dielectric fluid of the EDM process. The spark discharge gap of the tool electrode and the workpiece electrode is greatly increased. (Ref 8, 40-42). When the EDM process begins to create the discharge channel, the conductive powder particles are quickly arranged into bridges under the action of an electromagnetic field. As a result the spark dis-

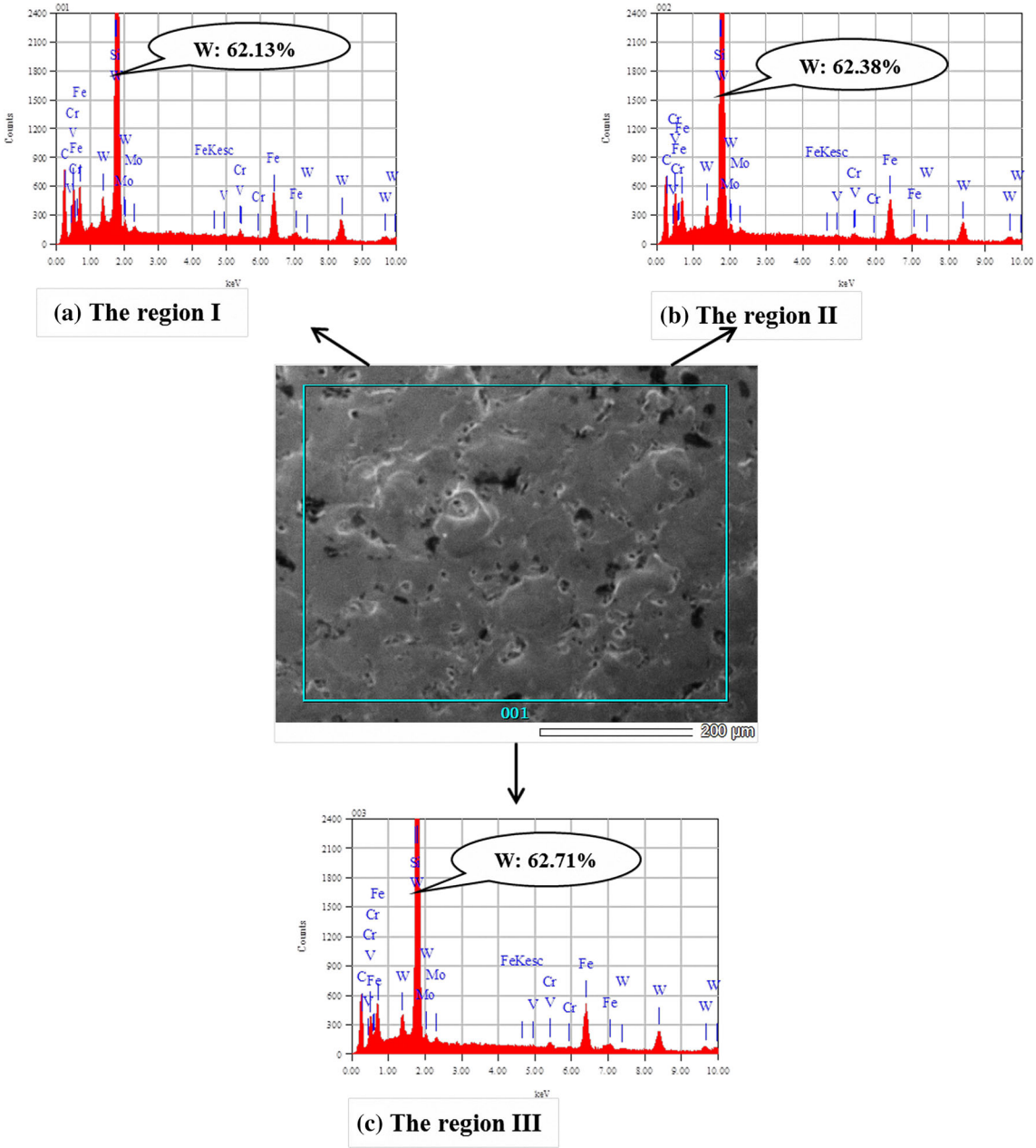


**Fig. 3** The content of the tungsten element in three different regions by EDX method at $I_p$ = 1 A; $T_{on}$ = 16 μs; $C_p$ = 60 g/l

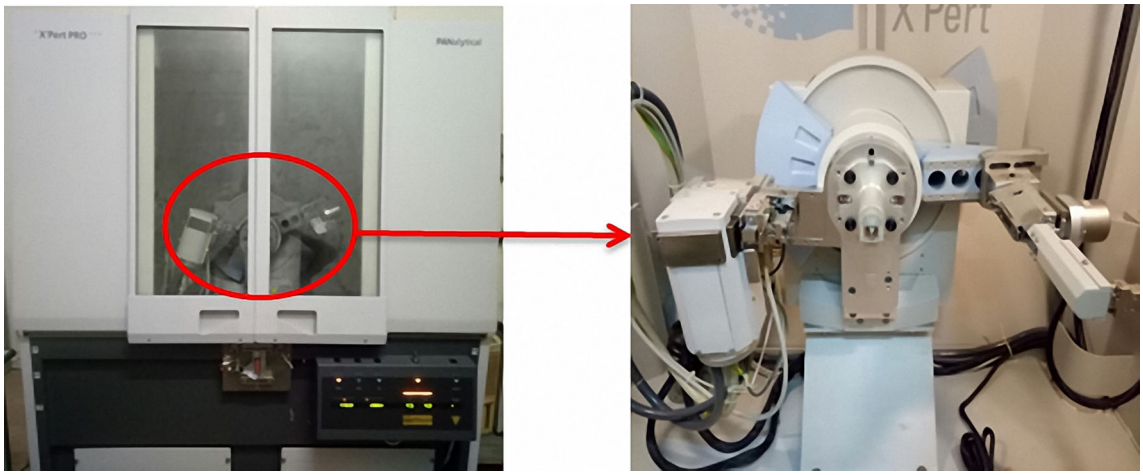

**Fig. 4** The x-ray diffraction of samples

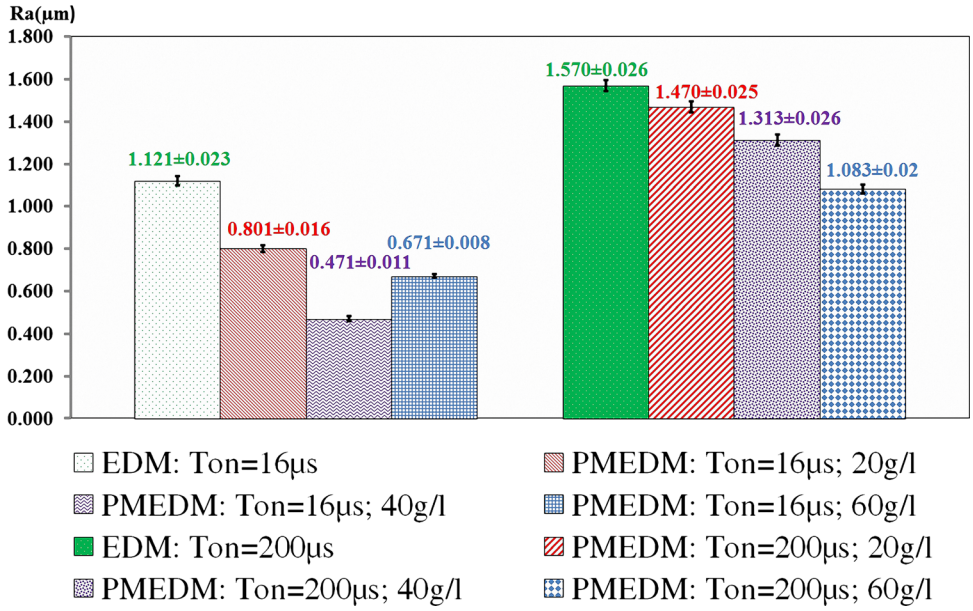


**Fig. 5** Average value and standard deviation of surface roughness at $I_p$ = 1 A

charge gap is increased. As the gap of the spark discharge increases, the energy of sparks is reduced. The result of MRR is reduced. So, the craters are created on the surface of workpieces, which are reduced depth and width (Ref 43, 44). This results in a reduced surface roughness. To justify this, Fig. 7 depicts the conductive powder particles, which are involved in the formation of the discharge channel.

b. Powder particles are taken part in the spark discharge process. Spark discharges are more uniform and the discharge channel is extended wider (Ref 8, 44). In the EDM process, the spark is created at one location, which have the smallest gap between the tool electrode and the workpiece electrode. But the PMEDM process, the conductive powder gives assistance to the formation of the discharge channel. This leads to the spark discharge at various locations, where the conductive powder created a bridge under the action of an electromagnetic field. The spark discharge process occurs at many locations on the surface of samples, create overlapping craters as shown in Fig. 8 and Ref 45. This leads to a decrease in the depth of craters as shows in Fig. 9. The arguments about the explanation of physical phenomena with the participation of powder particles as mentioned above, make it clearer about the improved surface roughness as compared to the surface roughness of the EDM process.

In Fig. 5 and 6, the surface roughness at $I_p$ = 1 A with all the pulse on time and the powder concentration is improved better than the surface roughness at $I_p$ = 4 with all the pulse on time and the powder concentration, respectively. In Fig. 5, at $I_p$ =1A; $T_{on}$ = 16 μs there is a good improvement of surface roughness as compared to that of $I_p$ = 1 A; $T_{on}$ = 200 μs with all concentration ranges. Fig. 6 ($I_p$ = 4 A) is also observed, it is similar to Fig. 5 ($I_p$ = 1 A), which have been mentioned above. According to Fig. 5, the surface roughness has the large reduction at $I_p$ = 1 A; $T_{on}$=16 μs with $C_p$=40 g/l; 60 g/l and as compared to other process parameters. However, in Fig. 6 the

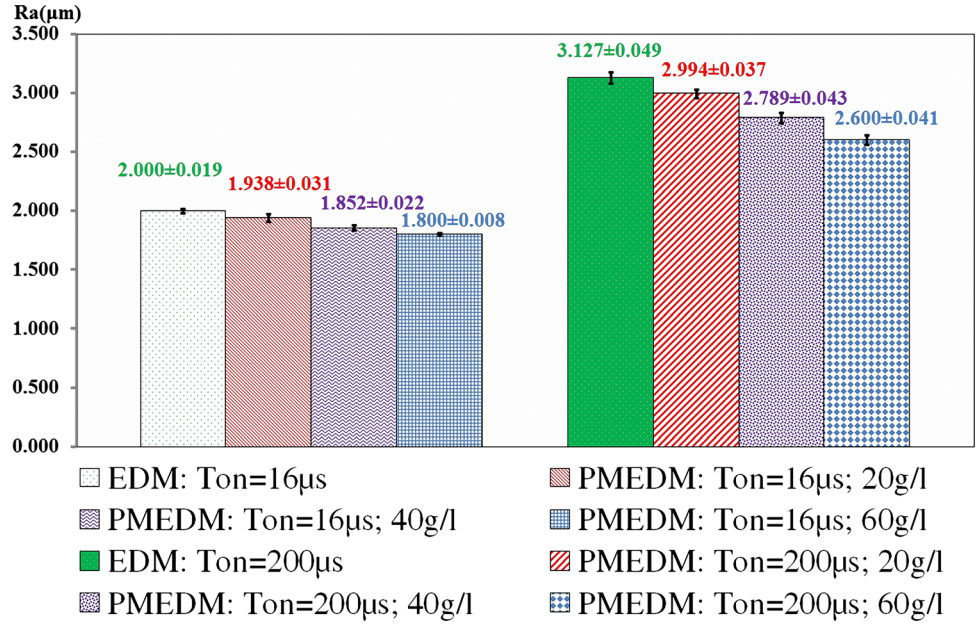


**Fig. 6** Average value and standard deviation of surface roughness at $I_p$ = 4 A

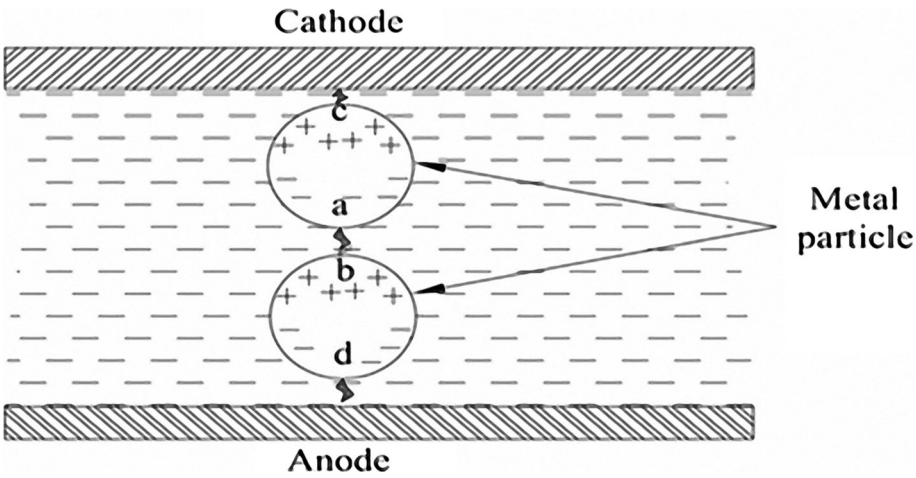


**Fig. 7** The spark discharge is created by the conductive powder (Ref 8)

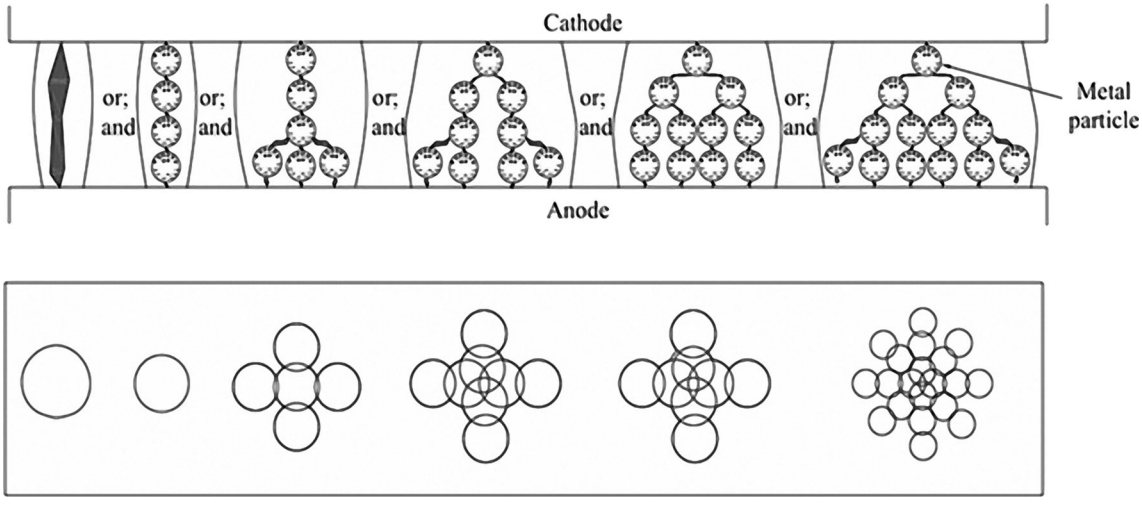


**Fig. 8** Proposing discharge process with the conductive powder in PMEDM

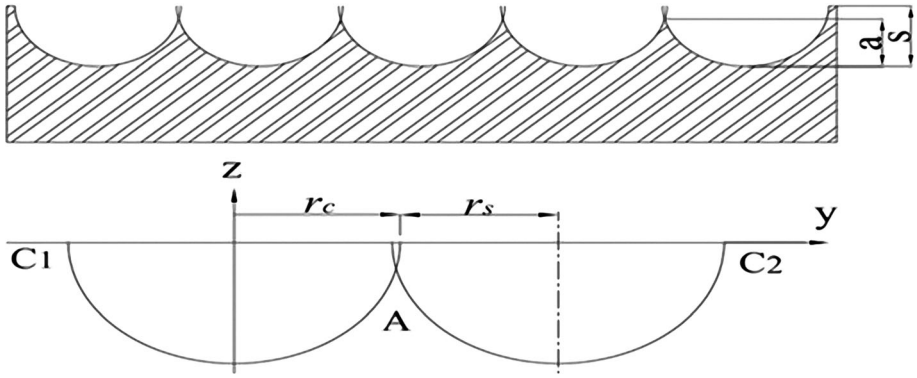


**Fig. 9** Mechanism of creating surface roughness (Ref 8, 46, 47)

surface roughness has the large reduction at $I_p$=4A; $T_{on}$=16μs with $C_p$=20 g/l; 60 g/l as compared to other process parameters. Observing Fig. 5 and 6, in Fig. 5 at $I_p$ = 1 A; $T_{on}$ = 16 μs; $C_p$ = 40 g/l has the surface roughness in $R_a$= 0.471 ± 0.011 μm. This is the best-improved surface roughness as compared to other process parameters, is a reduction of 57.984% as compared to the normal EDM. These phenomena are explained as follows: The peak current, the pulse on time, and the pulse off time are combined reasonably. This creates the broken pressure of the gas bubble in the previous spark discharge stage, which is small. This results in a high density of powder particles in the next discharge channel, supports the spark discharge process in aspects: The gap of spark discharge is increased. The spark discharge channel is expanded. As a result, the density of sparks is more even. Therefore, these are the main causes. The surface roughness by the PMEDM process is better than that of the EDM process.

In the opposite direction. Figure 5, and 6 concentrates on cases, in which surface roughness of the PMEDM process has a non-significant effect than that of the EDM process. In Fig. 5, at $I_p$ = 1 A; $T_{on}$ = 200 μs; $C_p$ = 20 g/l the surface roughness is 1.57 ± 0.026 μm. In comparison with the EDM process, the surface roughness has a reduction of 6.3%. Meanwhile, in Fig. 6, at $I_p$ = 4 A; $T_{on}$ = 200 μs; $C_p$ = 20 g/l the surface roughness has the smallest variation, a reduction of 4.25% as compared to that of the EDM process. The explanation for these phenomena: There is a mismatch of the peak current, the pulse on time, and the pulse off time. The broken pressure of the gas bubble in the previous spark discharge stage is big. This results in a low density of powder particles in the next discharge channel, not support the spark discharge process in aspects: The gap of spark discharge is reduced. The spark discharge channel is not expanded. As a result, the density of sparks is not uniform. Therefore, these are the main causes. The surface roughness of the PMEDM process is not better than the normal EDM process.

*The trend in the variation of surface roughness:* According to the graphs of Fig. 10 and 11, they show explicitly the influence trend of each process parameters on the surface roughness of samples. Comparing Fig. 10 and 11, the peak current $I_p$ = 1 A (Fig. 10) has a more positive effect than the peak current $I_p$ = 4 A (Fig. 11) in improved surface roughness of samples. In addition, according to Fig. 10, the pulse on time $T_{on}$ = 16 μs has a more positive effect than the pulse on time $T_{on}$ = 200 μs in improved surface roughness of samples. However, in Fig. 11, the pulse on time $T_{on}$ = 16 μs has an equal effect approximately as compared to the pulse on time $T_{on}$ = 200 μs in improved surface roughness of samples. Through the above analysis and evaluation, the role of powder particles is involved in the spark discharge process. They have a positive effect on improved surface roughness at the small peak current with the short pulse on time and the long pulse on time, not a positive effect on improved surface roughness at the large peak current with the short pulse on time and the long pulse on time.

### 3.2 Surface Morphology

Figure 12, 13, 14, and 15 generally describes the surface morphology of the machined samples by EDM process and PMEDM process. The ridges at the edge of the crater have been depicted in Fig. 12a. It is representative of Fig. 12, 13, 14, and 15. The high ridges at the edge of the crater have created a rough surface. In contrast, the low ridges at the edge of the crater have created a smooth surface. The ridges at the edge of the crater is the basis for evaluating surface morphology (Ref 18). As Fig. 16, 17, 18, and 19 describes the defects on machined surfaces by the EDM process and PMEDM process. The defects are described and indicated as Fig. 16 a. It is representative of Fig. 16, 17, 18, and 19.

In Fig. 12, 13, 14, and 15 were observed. Figures show that the surface morphology of samples by the PMEDM process has a smoothness, whereas the surface morphology of samples by the EDM process has a roughness. Thus, when the powder was added to the insulating dielectric fluid, the surface morphology has been improved. However, the effect of tungsten carbide powder on the improvement of surface morphology is more, or less. This is decided by the combination of the peak current, the pulse on time, and the powder concentration.

At $I_p$ = 1 A, Pulse on time is varied from 16 to 200 μs, as shown in Fig. 12, 13 and Fig. 16 and 17. In Fig. 12(b, c, d), 13(b, c, d), 16(b, c, d), and 17(b, c, d ), the surface morphology of machined samples by the PMEDM process has changed markedly in the smoothness of surfaces, micro-crack, void, droplet, globule of debris as compared to that of the EDM process as in Fig. 12a, 13a, 16a, and 17a. The surface smoothness of machined samples by the PMEDM process is usually better than that of machined samples by the EDM process. The micro-cracks, voids, droplets, and globules of debris on the surface of machined samples by the PMEDM process usually appear less as compared to that of the EDM process. The phenomenon is due to the participation of conductive powder particles. They have improved the spark discharge process, reduced the insulation of dielectric fluid,

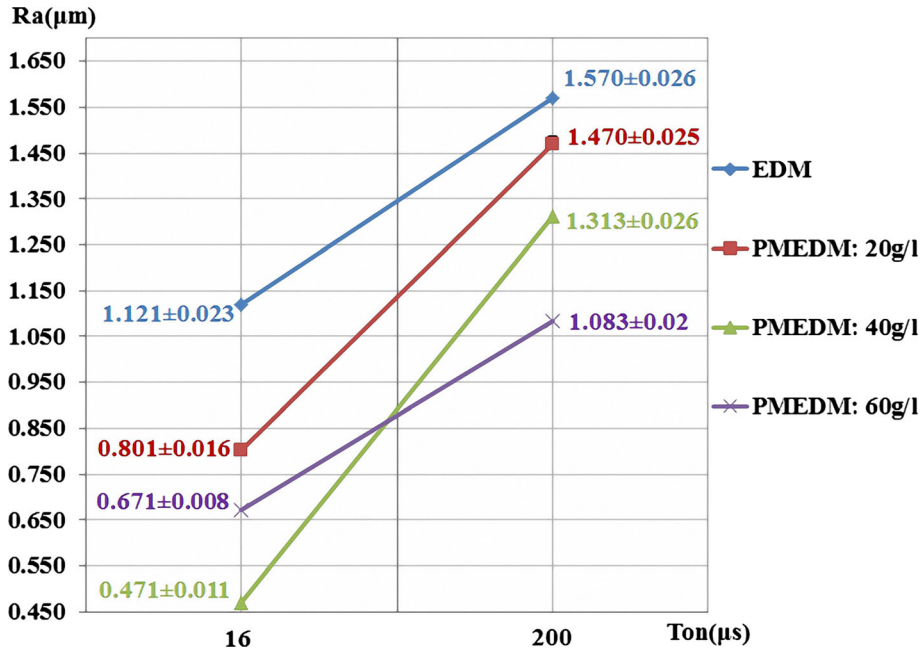


**Fig. 10** The trend of surface roughness at $I_p$ = 1 A

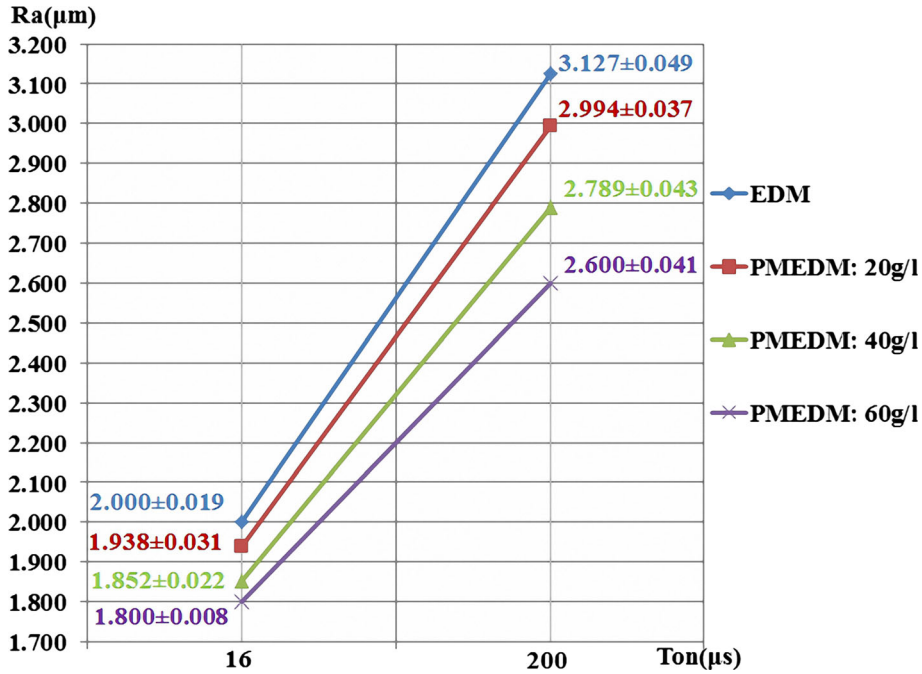


**Fig. 11** The trend of surface roughness at $I_p$ = 4 A

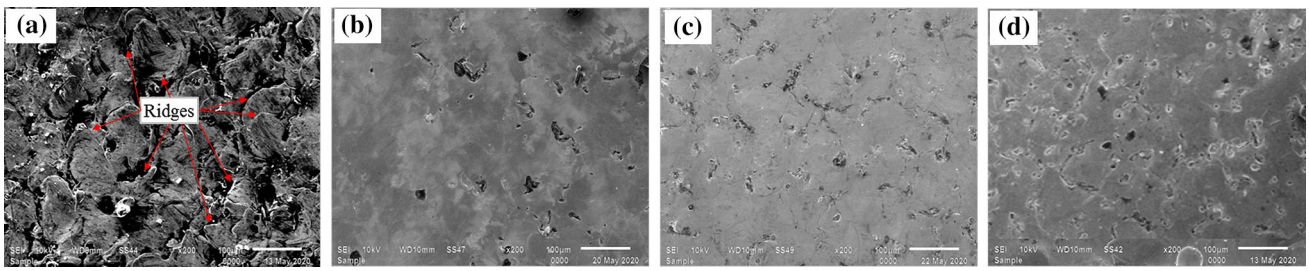


**Fig. 12** Surface morphology at $I_p$ = 1 A; $T_{on}$ = 16 µs: (a) $C_p$ = 0 g/l; (b) $C_p$ = 20 g/l; (c) $C_p$= 40 g/l; (d) $C_p$ = 60 g/l

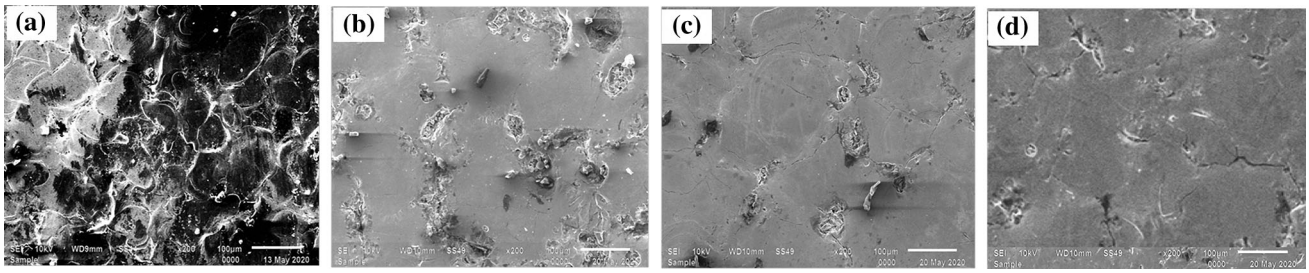


**Fig. 13** Surface morphology at $I_p$ = 1 A; $T_{on}$ = 200 µs: (a) $C_p$ = 0 g/l; (b) $C_p$ = 20 g/l; (c) $C_p$= 40 g/l; (d) $C_p$ = 60 g/l

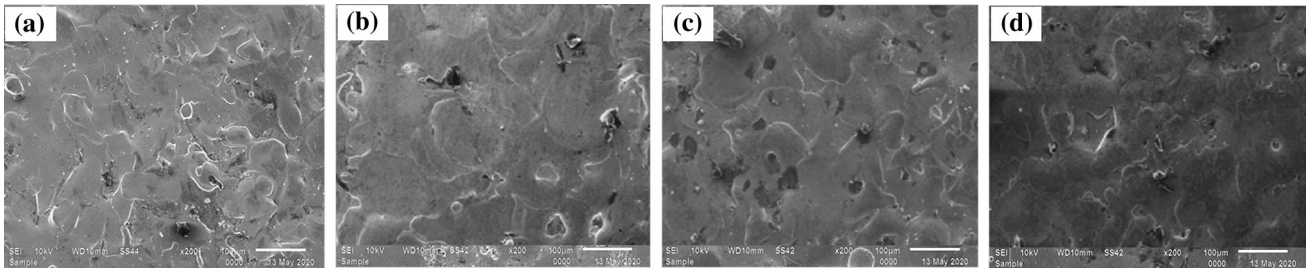


**Fig. 14** Surface morphology at $I_p$ = 4 A; $T_{on}$ = 16 µs: (a) $C_p$ = 0 g/l; (b) $C_p$ = 20 g/l; (c) $C_p$ = 40 g/l; (d) $C_p$ = 60 g/l

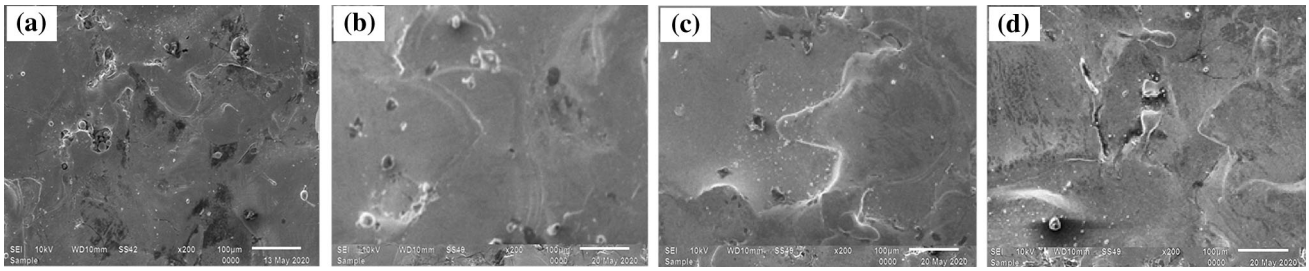


**Fig. 15** Surface morphology at $I_p$ = 4 A; $T_{on}$ = 200 µs: (a) $C_p$ = 0 g/l; (b) $C_p$ = 20 g/l; (c) $C_p$ = 40 g/l; (d) $C_p$ = 60 g/l

reduced the viscosity of dielectric fluid, and enhanced the ability to transfer heat to the outside environment (Ref 48, 49). In Fig. 13(b, c, d), 17(b, c, d), the surface morphology of samples at $T_{on}$ = 200 µs, including the smoothness of surfaces, micro-crack, void, droplet, globule of debris has not improved much as compared to the surface morphology of the sample at $T_{on}$ = 16 µs as Fig. 12(b, c, d), 16(b, c, d). The phenomenon of the surface morphology at $T_{on}$ = 200 µs has not improved much as compared to the surface morphology at $T_{on}$=16 µs with all concentrations. Because, at $T_{on}$ = 200µs has produced a large discharge energy. This results in a large amount of material removal on surface of samples. However, the pulse off time ($T_{off}$ = 50 µs) is not enough time to eject all debris from the discharge area of the previous spark discharge. As a result, some debris has adhered on the surface and suspended in the dielectric liquid. This has formed the unstable discharge process of the next time (Ref 50), created defects on the surface. In addition, there is a mismatch of the peak current, the pulse on time, and the pulse off time. The broken pressure of the gas bubble in the previous spark discharge stage is big. This results in a low density of powder particles in the next discharge channel, not support the spark discharge process. This has formed the surface morphology as in Fig. 13(b, c, d), 17(b, c, d). In contrast, the pulse on time $T_{on}$ = 16 µs has produced a discharge energy, which is less than the discharge energy at $T_{on}$ = 200 µs. Hence, the amount of material removal on the surface of samples at $T_{on}$ = 16 µs is less than the amount of material removal on the surface of samples at $T_{on}$ = 200 µs. With the pulse off time ($T_{off}$ = 50 µs) is enough time to eject most of the debris from the discharge area of the previous spark discharge. As a result, few debris has adhered and created fewer defects on the surface. In addition, the peak current, the pulse on time, and the pulse off time are combined reasonably. This creates the broken pressure of the gas bubble in the previous spark discharge stage, which is small. This results in a high density of powder particles in the next discharge channel, supports well the spark discharge process. This has formed the surface morphology as in Fig. 12(b, c, d), 16(b, c, d). Powder concentration is varied from 20 g/l to 60 g/l. As a result, the surface morphology has also changed in a positive direction. The surface of samples is smoother, fewer defects. The results of the observation showed that the sample has the best improvement in surface morphology at $I_p$ = 1 A, $T_{on}$ = 16 µs, $C_p$ = 60 g/l. Because it has a smooth surface, few micro-cracks, few voids, few droplets, few globules of debris.

In Fig. 14, 15, 18 and 19, at $I_p$=4A, pulse on time is varied from 16 µs to 200 µs. In Fig. 14(b, c, d), 18(b, c, d ), the surface morphology of machined samples by the PMEDM process has changed in the smoothness of surfaces, micro-crack, void, droplet, globule of debris as compared to that of the EDM

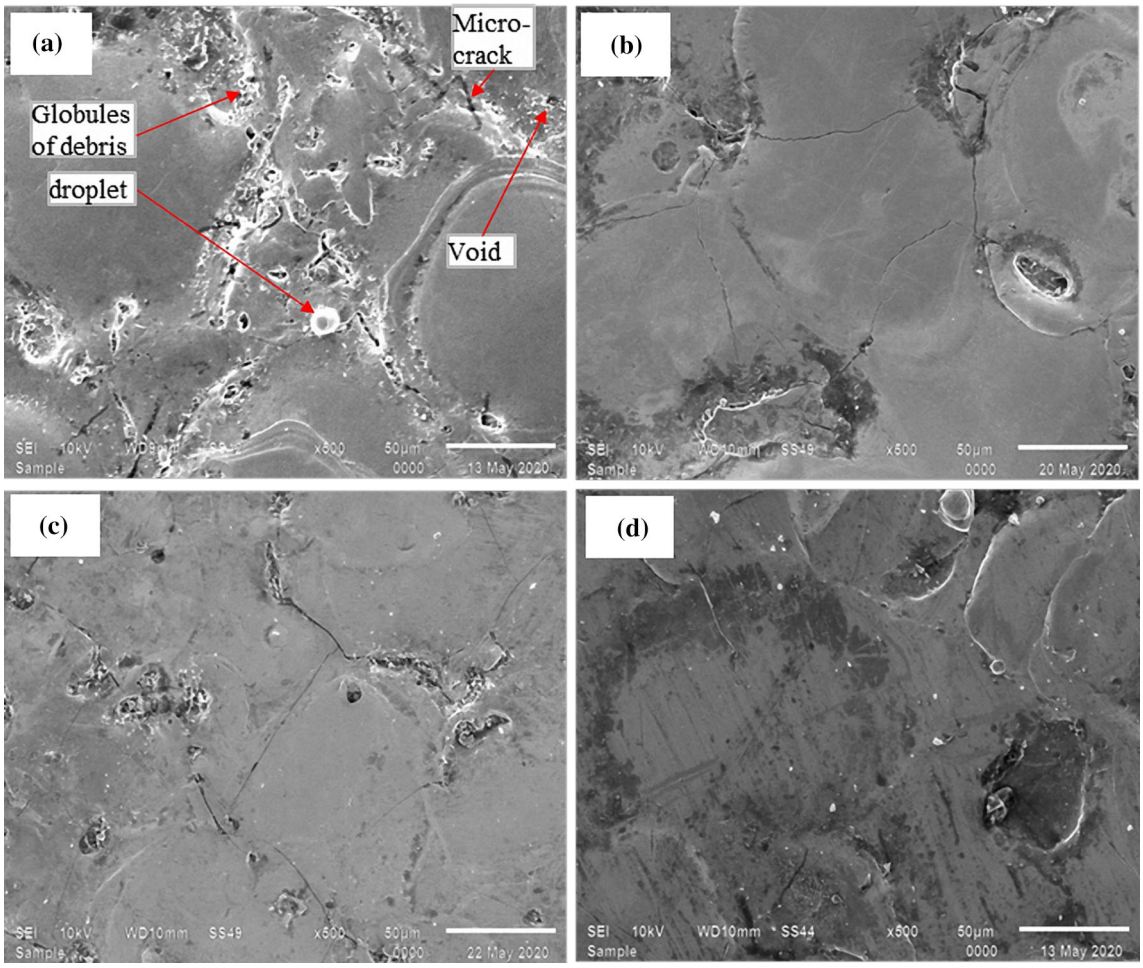


**Fig. 16** Microdefects on the surface at $I_p$ = 1 A; $T_{on}$ = 16 µs: (a) $C_p$ = 0 g/l; (b) $C_p$ = 20 g/l; (c) $C_p$ = 40 g/l; (d) $C_p$ = 60 g/l

process as in Fig. 14a, 18a. The surface smoothness of machined samples by the PMEDM process is usually better than that of machined samples by the EDM process. The micro-cracks, voids, droplets, and globules of debris on the surface of machined samples by the PMEDM process usually appear less as compared to that of the EDM process. The phenomenon is due to the participation of conductive powder particles. They have improved the spark discharge process, reduced the insulation of dielectric fluid, reduced the viscosity of dielectric fluid, and enhanced the ability to transfer heat to the outside environment (Ref 48, 49). However, in Fig. 15(b, c, d), 19(b, c, d), the surface morphology of machined samples by the PMEDM process has not changed more in the smoothness of surfaces, micro-crack, void, droplet, globule of debris as compared to that of the EDM process. The main reason, at $I_p$ = 4 A, $T_{on}$ = 200 µs are larger and longer, respectively. This has produced a large discharge energy, the expansion of the plasma channel in the discharge process. As a result, the broken pressure of the gas bubble in the previous spark discharge is large. Resulting in very little or no powder particles has been involved in the next discharge process. This has not improved the spark discharge process, reduced the insulation of dielectric fluid, reduced the viscosity of dielectric fluid, and enhanced the ability to transfer heat to the outside environment. Moreover, with large electrical process parameters as $I_p$ = 4 A, $T_{on}$ = 200 µs. This has produced a large amount of material removal on surface of samples. However, the pulse off time ($T_{off}$ = 50 µs) is not enough time to eject all debris from the discharge area of the previous spark discharge. As a result, some debris has adhered, created defects on the surface. This has formed the surface morphology as in Fig. 15(b, c, d), 19(b, c, d). Powder concentration is varied from 20 g/l to 60 g/l. As a result, the surface morphology has also changed in a less positive direction. The surface of samples is smooth less, not good in the improvement of defects.

In Fig. 14(b, c, d), 15(b, c, d) and 18(b, c, d), 19(b, c, d) is the surface morphology of $I_p$ = 4 A with the variation of pulse on time from 16 to 200 µs and powder concentration from 20 g/l to 60 g/l. They are improved less than the surface morphology of $I_p$ = 1 A with the variation of pulse on time from 16 to 200 µs and powder concentration from 20 to 60 g/l, respectively. When this machined surface morphology with powder is compared to the surface morphology by the normal EDM process. Because at $I_p$ = 4 A, this has produced a large discharge energy, the expansion of the plasma channel in the discharge process. As a result, the broken pressure of the gas bubble in the previous spark discharge is large. Resulting in very little or no powder particles has been involved in the next discharge process. This has not improved the spark discharge process, reduced the insulation of dielectric fluid, reduced the viscosity of dielectric fluid, and enhanced the ability to transfer heat to the outside environment.

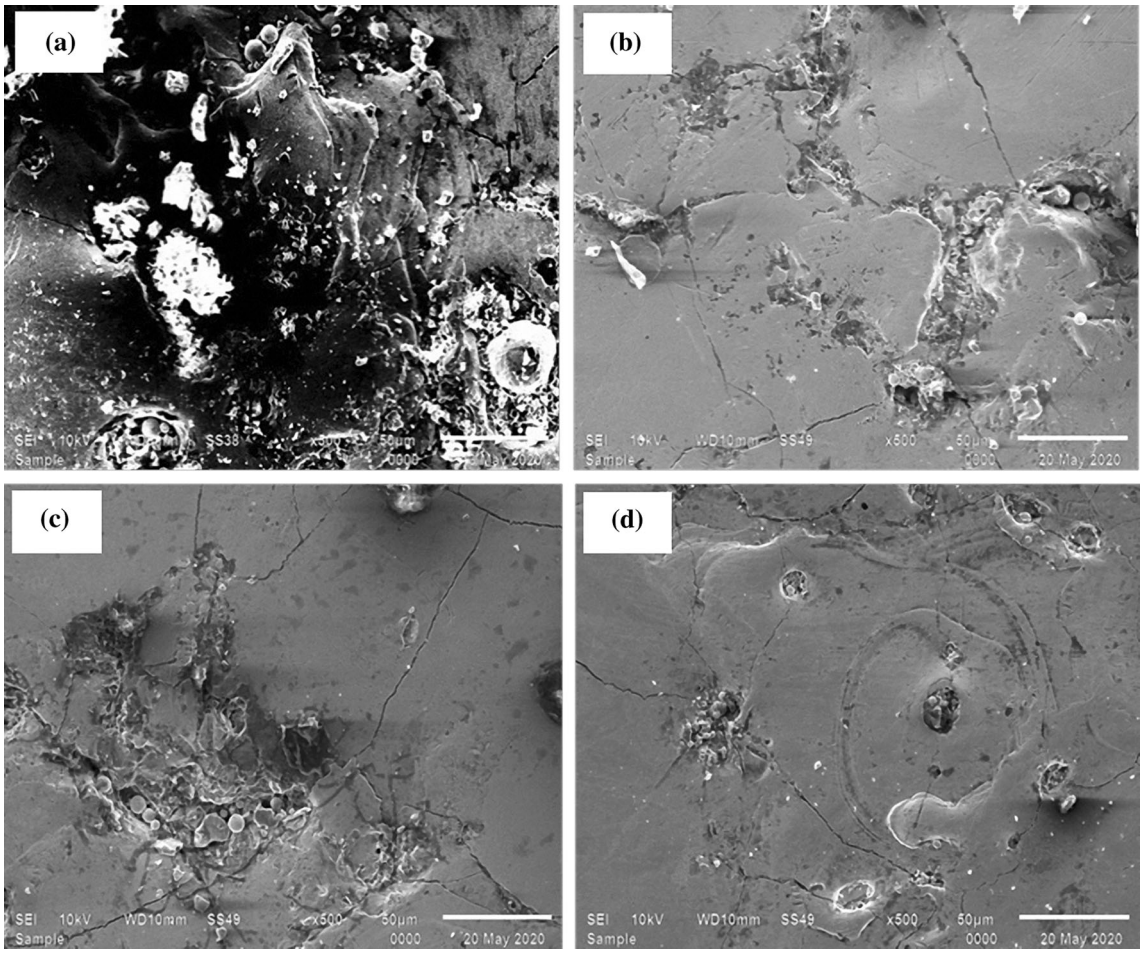


**Fig. 17** Microdefects on the surface at $I_p$ = 1 A; $T_{on}$ = 200 µs: (a) $C_p$ = 0 g/l; (b) $C_p$ = 20 g/l; (c) $C_p$ = 40 g/l; (d) $C_p$ = 60 g/l

### 3.3 Microhardness of Surfaces

According to Fig. 20 and 21, the microhardness on surfaces of machined samples by the PMEDM process is higher than that of the EDM process at the various main process parameters in all the experiments. However, at $I_p$ = 4 A, $T_{on}$ = 200 µs, and $C_p$ = 60 g/l the microhardness is approximately equal to the microhardness of machined surfaces by the EDM process with the same electrical process parameters (according to Fig. 21). At $I_p$ = 1 A (as Fig. 20) with the variation of pulse on time from 16 to 200 µs, the microhardness on surfaces of $T_{on}$ = 16 µs is improved better than the microhardness on surfaces of $T_{on}$ = 200 µs with the variation of powder concentration from 20 to 60 g/l, respectively. At $I_p$ = 1 A, $T_{on}$ = 16 µs and $T_{on}$ = 200 µs, the powder concentration is increased from 20 to 60 g/l, the microhardness on surfaces is also increased in proportion to the powder concentration. However, at $I_p$ = 1 A and $T_{on}$ = 200 µs, the variation amplitude of microhardness on surfaces increases not much when the powder concentration changes from 20 to 60 g/l. At $I_p$ = 4 A (as Fig. 21) with the variation of pulse on time from 16 to 200 µs, the microhardness on surfaces of $T_{on}$=16 µs is improved better than the microhardness on surfaces of $T_{on}$=200 µs with the variation of powder concentration from 20 to 60 g/l, respectively. At $I_p$ = 4 A, $T_{on}$ = 16 µs the powder concentration is increased from 20 to 60 g/l, the microhardness on surfaces is not significantly increased. Even, the microhardness on surfaces of $C_p$ = 40 g/l is reduced as compared with the microhardness on surfaces of $C_p$ = 20 g/l. At $I_p$=4 A, $T_{on}$ = 200 µs the powder concentration is increased from 20 to 40 g/l, the microhardness on surfaces is increased. However, the microhardness on surfaces of $C_p$ = 60 g/l is reduced as compared with the microhardness on surfaces of $C_p$ = 20 g/l and 40 g/l. Based on the experimental data about the microhardness on surfaces is analyzed and evaluated. At $T_{on}$ = 16 µs; $I_p$ = 1 A and $C_p$ = 60 g/l the highest microhardness of surfaces is 825 ± 19 HV as Fig. 20, increased 129.167% as compared to the microhardness on surfaces of the normal EDM process.

### 3.4 The Explanation for the Phenomenon of Varied Microhardness

a. The participation of powder particles in the EDM process has made the variation of surface microhardness. To further clarify this phenomenon. The tungsten element penetration into the workpiece surface after machining has been investigated by EDX method. The percentage of the tungsten element is shown in Fig. 22 and 23. Tungsten element has existed on the surface of samples. However, not all surfaces of the samples have the tungsten element. The content of the tungsten element is more or less, which depends on the combination of main process

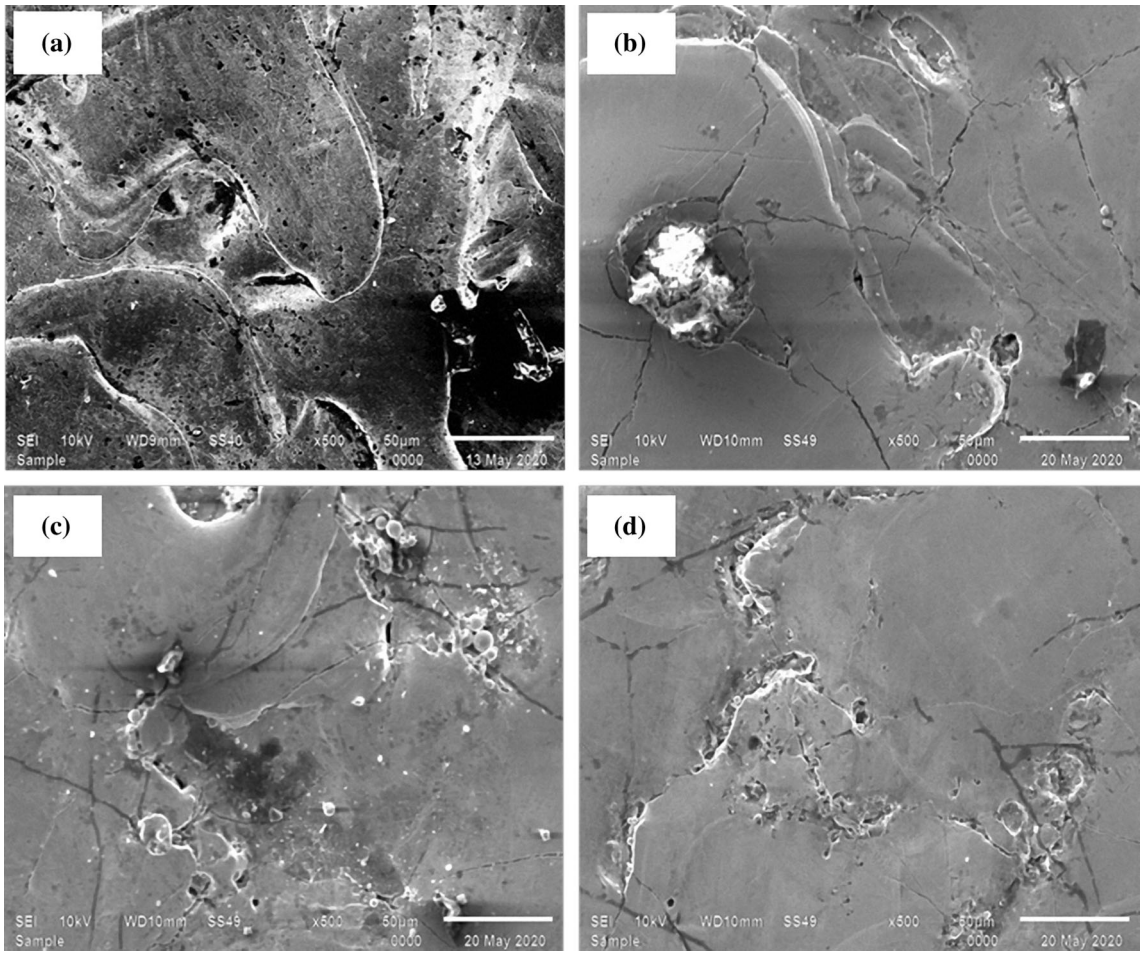


**Fig. 18** Microdefects on the surface at $I_p$ = 4 A; $T_{on}$=16 µs: (a) $C_p$ = 0 g/l; (b) $C_p$ = 20 g/l; (c) $C_p$ = 40 g/l; (d) $C_p$ = 60 g/l

parameters as in Fig. 22 and 23. The above result is due to the penetration of the tungsten element into the surface of samples. This penetration of the tungsten element is assisted by the heat channel, which was formed in the spark discharge process. The tungsten element of tungsten carbide powder is united with the carbon element in the dielectric fluid or the internal carbon element in the surface of workpieces under the heat effect of the EDM process. Hence, the tungsten carbide has been formed in the circumstances of the above—mentioned. In addition, the tungsten carbide in the powder is melted, evaporated, and penetrated into the surface of the workpieces. Therefore, the microhardness of the surface has been improved. According to Fig. 24, the tungsten carbide phase has been confirmed by XRD method, which explains the phenomenon of the microhardness of surfaces by PMEDM process higher than the microhardness of surfaces by EDM process. Consequently, the process of electrical discharge has generated heat to melt the tungsten carbide powder, other compounds of the dielectric fluid, and other compounds of the SKD61 material of the samples. This has led to the penetration of some chemical elements into surfaces, which include tungsten and tungsten carbide. The penetration of tungsten and tungsten carbide into the surface is explained by phenomena (Ref 2, 18, 48, 51) as: Those are the process of diffusion including microscopic diffusion, the process of chemical reactions, the evaporation, adsorption of physical processes, and the mechanical adhesion process.

b. The microhardness of surfaces by the PMEDM process is approximately equal to the microhardness of surfaces by the EDM process. This phenomenon is due to the formation of thermal channels in the PMEDM process, which has created low thermal channels. This has not created the penetration of tungsten, tungsten carbide, and other compounds into surfaces. Another reason is due to the low content of tungsten on surfaces according to Fig. 22, and 23, which makes the appearance of the tungsten carbide phase is low, and unevenly distributed. In addition, the high concentration of tungsten carbide powder in the process of spark discharges leads to instability in the spark discharge process. This leads to the formation of

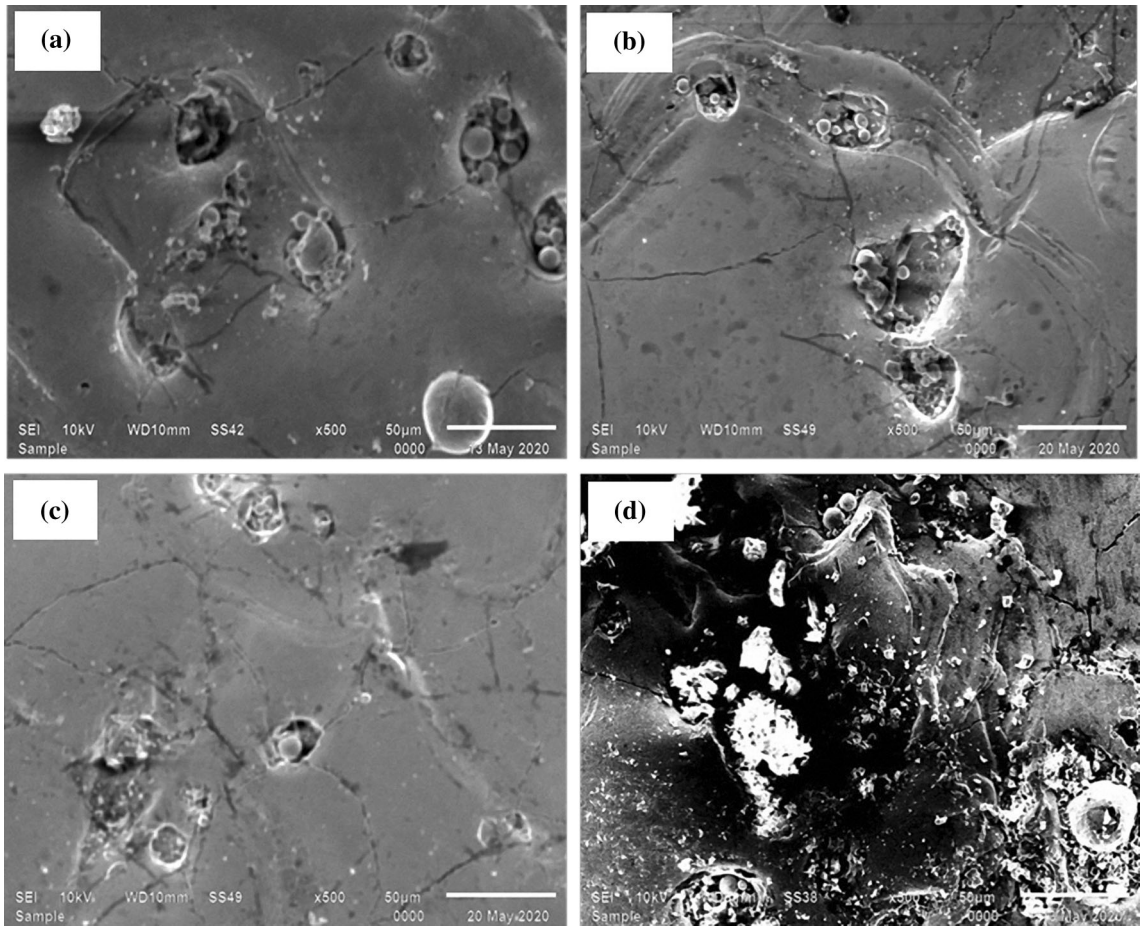


**Fig. 19** Microdefects on the surface at $I_p$ = 4A; $T_{on}$ = 200 µs: (a) $C_p$ = 0 g/l; (b) $C_p$ = 20 g/l; (c) $C_p$ = 40 g/l; (d) $C_p$ = 60 g/l

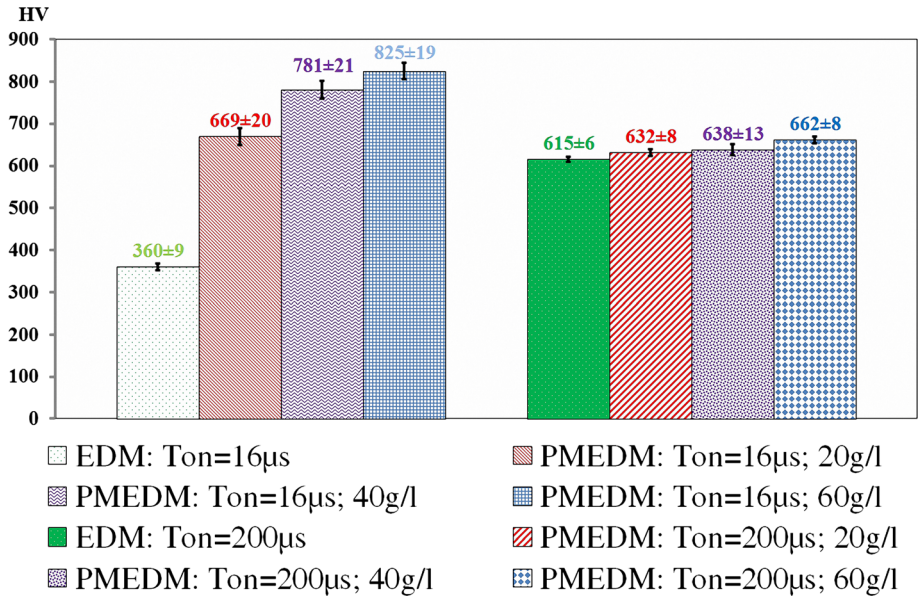


**Fig. 20** Average value and standard deviation of surface microhardness at $I_p$ = 1 A

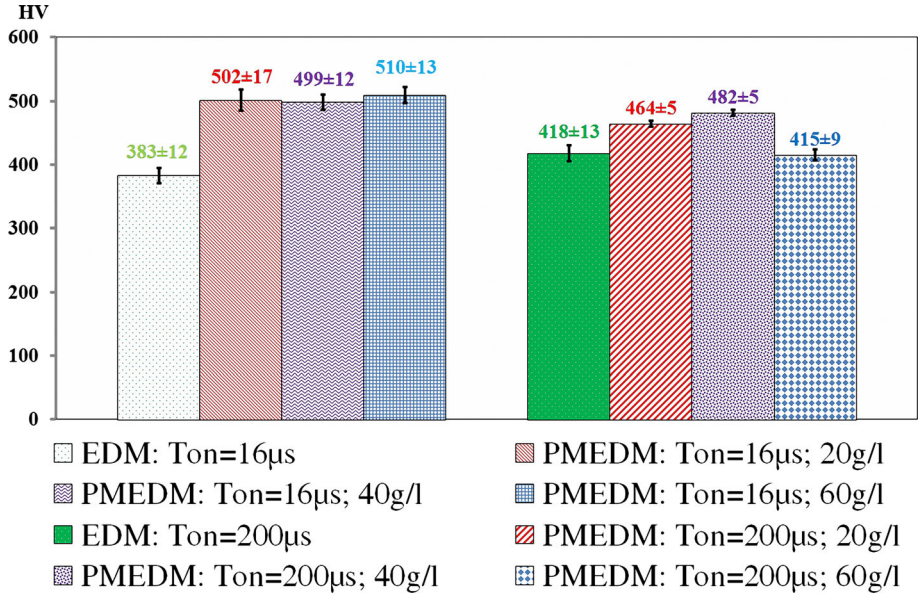


**Fig. 21** Average value and standard deviation of surface microhardness at $I_p$ = 4 A

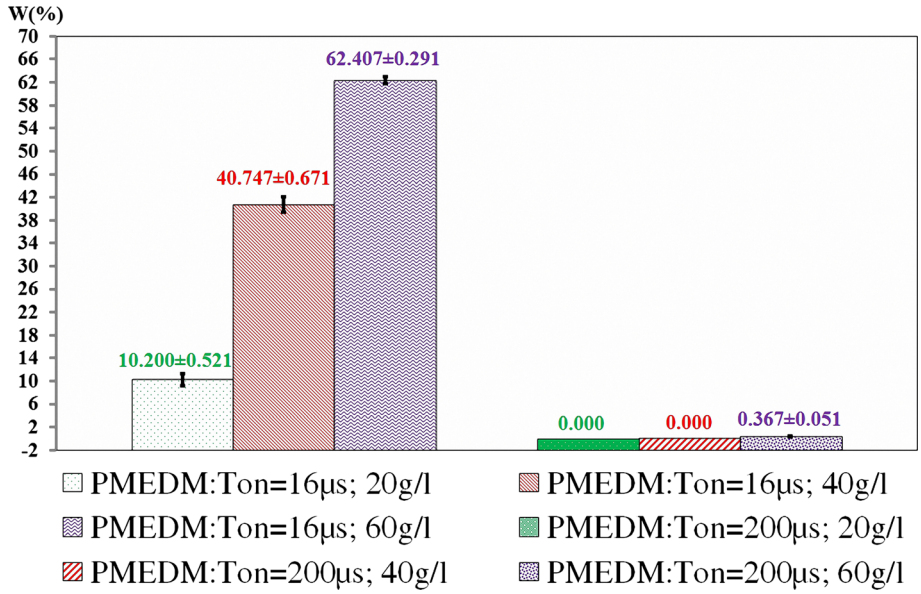


**Fig. 22** Tungsten content on the surface and standard deviation at $I_p$ = 1 A

electrical arcing and short circuit (Ref 41). This is also the cause of the formation of the low heat channel, which is not assisted to form the penetration of the tungsten, tungsten carbide, and other compounds into surfaces.

### 3.5 The Trend of the Tungsten Penetration into the Surface of Samples

As observed in Fig. 25 and 26, it is found that the penetration of the tungsten element into surfaces of samples at

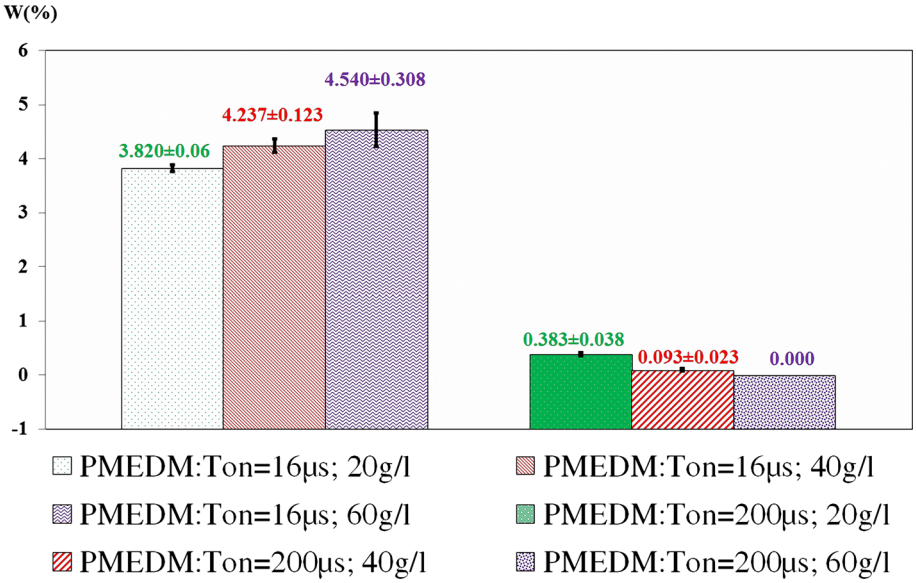


**Fig. 23** Tungsten content on the surface and standard deviation at $I_p$ = 4 A

$I_p$ = 1 A; 4 A, and the short pulse on time ($T_{on}$ = 16 μs) is better than the penetration of the tungsten element into surfaces of samples at $I_p$ = 1 A; 4 A, and the long pulse on time ($T_{on}$ = 200 μs) with all concentrations. Moreover, according to Fig. 25 and 26 the penetration of the tungsten element into surfaces of samples at the small peak current ($I_p$ = 1 A) and the short pulse on time ($T_{on}$ = 16 μs) is better than that at the large peak current ($I_p$ = 4 A) and the short pulse on time ($T_{on}$ = 16 μs) with all concentrations. The best result is 62.407 ± 0.291% of tungsten in surfaces at $T_{on}$ = 16 μs; $I_p$ = 1 A; $C_p$ = 60 g/l.

### 3.6 The Trend of the Microhardness Improvement on the Surface of Samples

As shown in Fig. 27 and 28, it is found that the improved microhardness on the surface of samples at $I_p$ = 1 A; 4 A and the short pulse on time ($T_{on}$ = 16 μs) is better than that at $I_p$ = 1 A; 4 A and the long pulse on time ($T_{on}$ = 200 μs) with all concentrations. Moreover, in Fig. 27, 28 the improved microhardness on the surface of samples at $I_p$ = 1 A and the short pulse on time ($T_{on}$ = 16 μs) is better than that at $I_p$ = 4 A and the short pulse on time ($T_{on}$ = 16 μs) with all concentrations. The highest microhardness on the surface is 825 ± 19 HV, improved by 129.167% as compared to the microhardness on surfaces of the normal EDM process at $T_{on}$ = 16 μs; $I_p$ = 1 A and $C_p$ = 60 g/l.

## 4. Conclusions

In this research, the influence trend of main process parameters including peak current, pulse on time, and tungsten carbide powder concentration on surface properties including surface roughness, microhardness of surfaces, and surface morphology has been investigated. A strategy for main process parameters was selected to analyze the influence of change in surface properties. The main results of this research can be summarized as follows:

- *Surface roughness:* The role of powder particles in the spark discharge process at $I_p$ = 1 A has a positive effect on the improvement of the surface roughness than that at $I_p$ = 4 A with all pulse on time and powder concentrations. At $I_p$ = 1 A and $T_{on}$ = 16 μs has a positive effect on the improvement of the surface roughness than that at $I_p$ = 1 A and $T_{on}$ = 200 μs with all powder concentrations. The best improvement of the surface roughness is $R_a$= 0.471 ± 0.011 μm with a reduction of 57.984% as compared to the normal EDM at $I_p$ = 1 A; $T_{on}$ = 16 μs; $C_p$ = 40 g/l.
- *Surface morphology:* The improved surface morphology at $I_p$ = 1 A is better than that at $I_p$ = 4 A with all pulse on time and powder concentrations. The improved surface

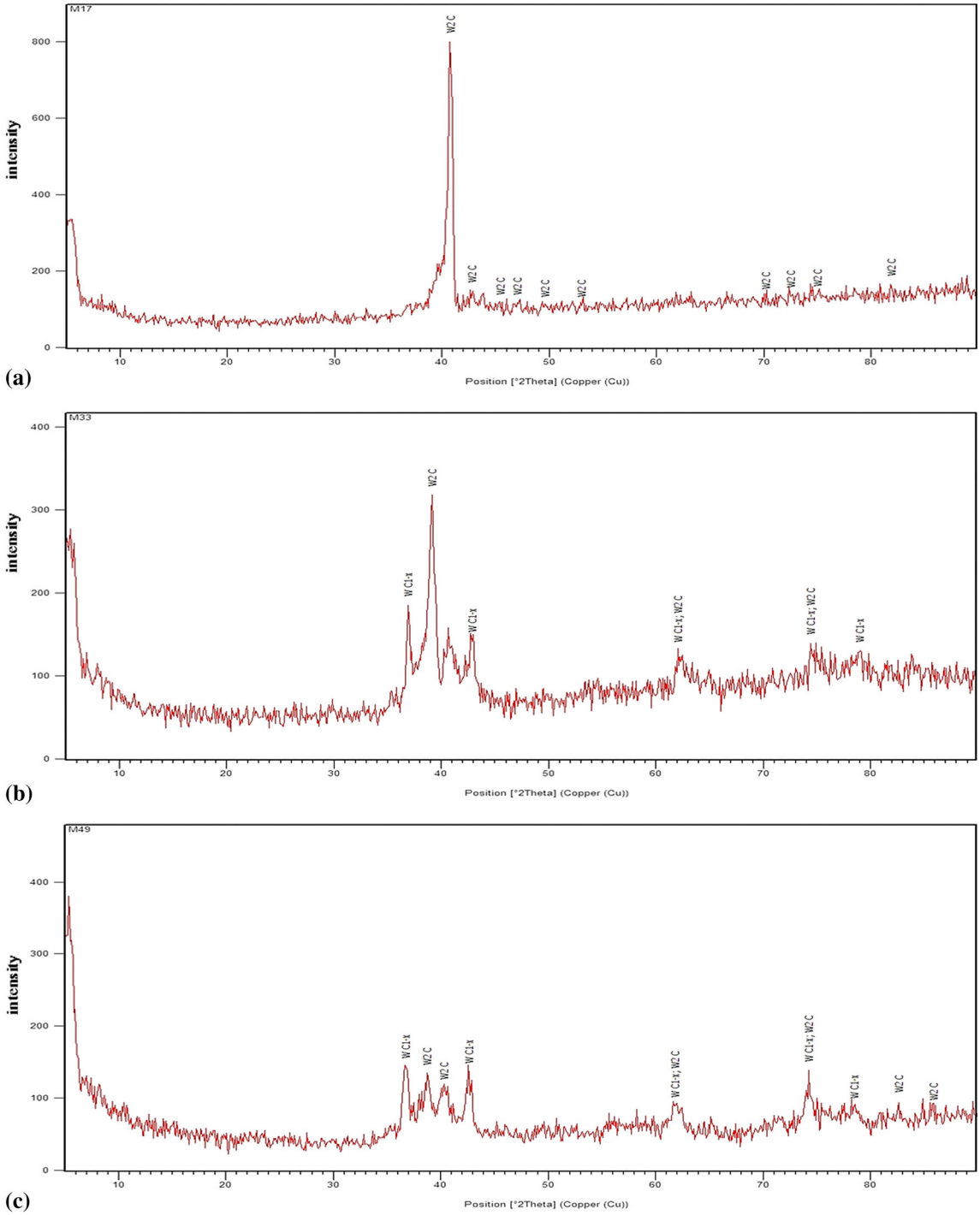


**Fig. 24** XRD analysis of the tungsten carbide phase: a) sample at $I_p$ = 1 A, $T_{on}$=16 µs, $C_p$ = 20 g/l; (b) sample at $I_p$ = 1 A, $T_{on}$ = 16 µs, $C_p$ = 40 g/l; (c) sample at $I_p$ = 1 A, $T_{on}$ = 16 µs, $C_p$ = 60 g/l

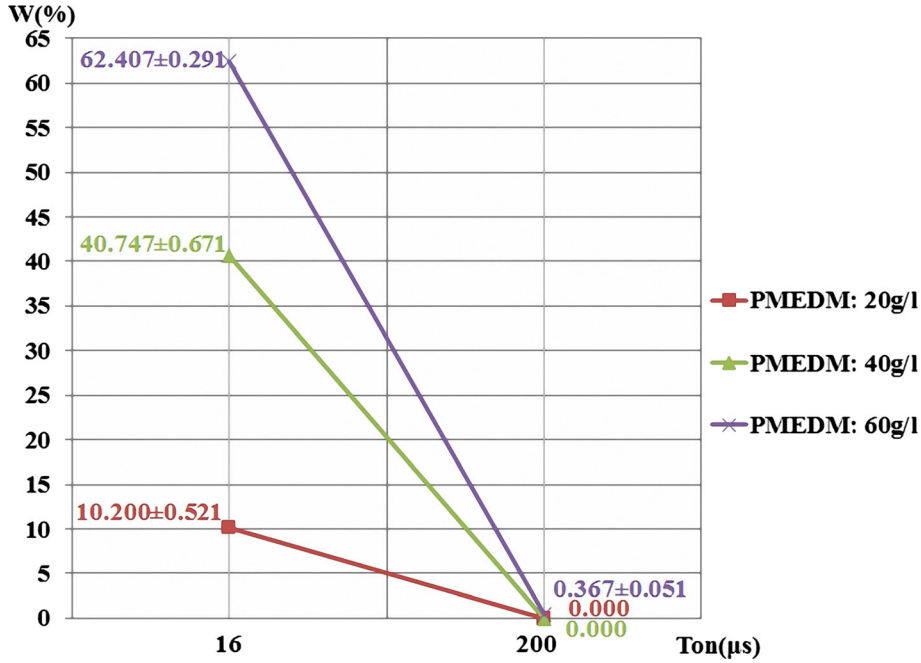


**Fig. 25** The trend of tungsten on the surface of workpieces at $I_p$ = 1 A

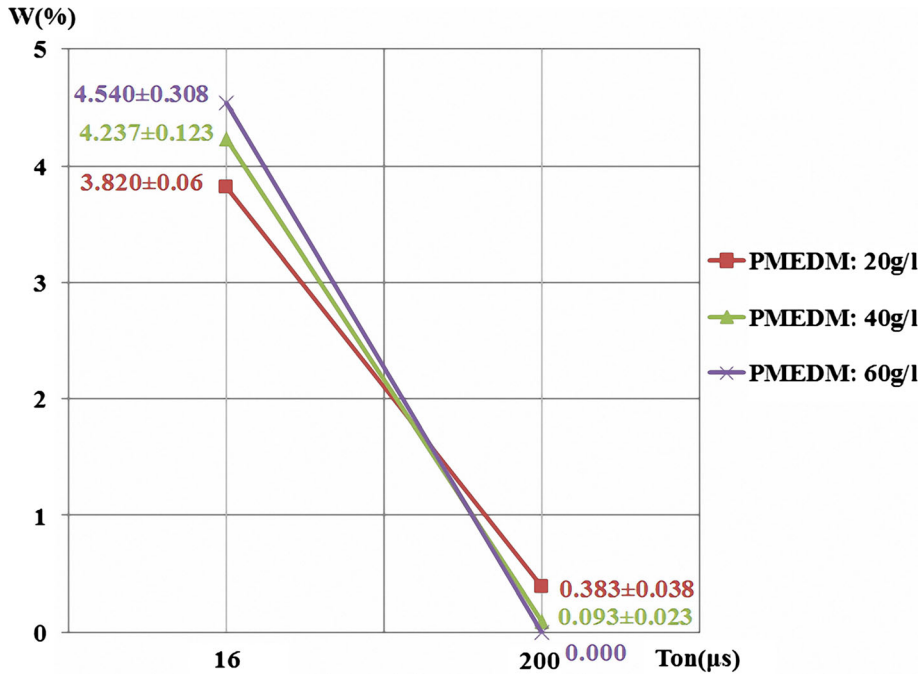


**Fig. 26** The trend of tungsten on the surface of workpieces at $I_p$ = 4 A

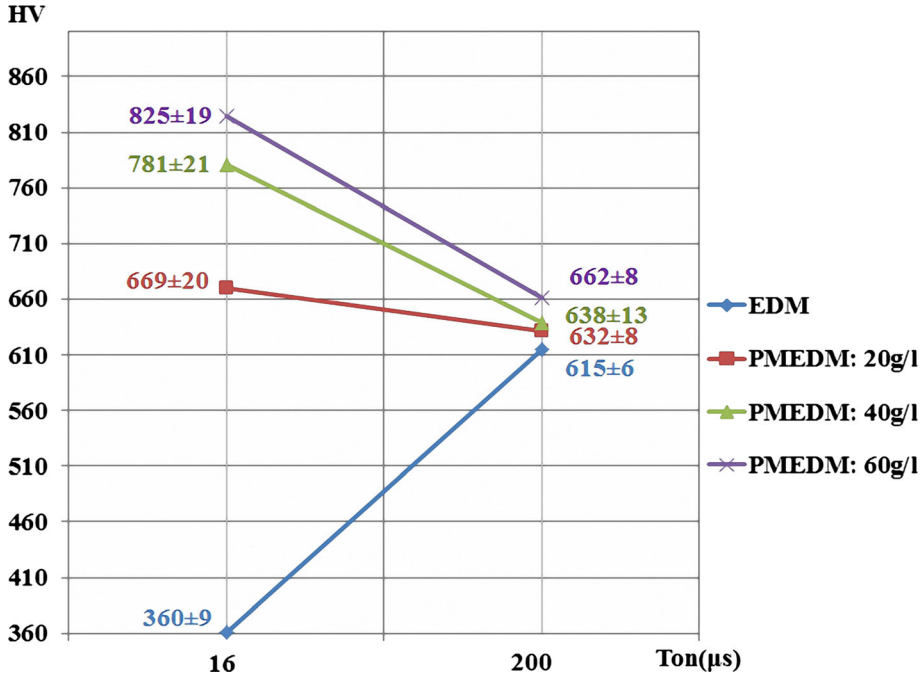


**Fig. 27** The trend of microhardness at $I_p$ = 1 A

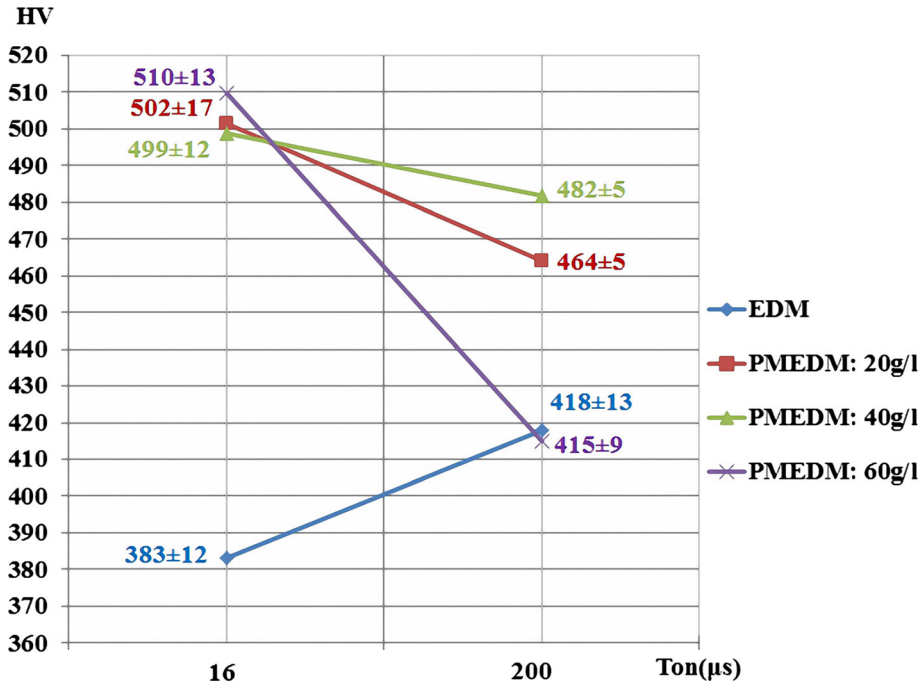


**Fig. 28** The trend of microhardness at $I_p$ = 4 A

morphology at $I_p$ = 1 A and $T_{on}$ = 16 µs is better than that at $I_p$ = 1 A and $T_{on}$ = 200 µs with all powder concentrations. The sample at $I_p$ = 1 A; $T_{on}$ = 16 µs; $C_p$ = 60 g/l has the best improvement in surface morphology, namely the smooth surface, the few micro-cracks, the few voids, the few droplets, and the few globules of debris compared to that of other process parameters and EDM process.

- *Microhardness:* The improved microhardness on surfaces at $T_{on}$ = 16 µs is better than that at $T_{on}$ = 200 µs with all peak current and powder concentrations. The improved microhardness on surfaces at $I_p$ = 1 A and $T_{on}$ = 16 µs is better than that at $I_p$ = 4 A and $T_{on}$ = 16 µs with all concentrations. The highest microhardness on the surface at $T_{on}$ = 16 µs; $I_p$ = 1 A; $C_p$ = 60 g/l is 825 ± 19 HV, improved by 129.167% as compared to the microhardness on surfaces of the normal EDM process.

## References


1. K. Furutani, A. Saneto, H. Takezawa, N. Mohri and H. Miyake, Accretion of Titanium Carbide by Electrical Discharge Machining with Powder Suspended in Working Fluid, *Precis. Eng.*, 2001, **25**, p 138–144. https://doi.org/10.1016/S0141-6359(00)00068-4
2. C. Prakash, H.K. Kansal, B.S. Pabla, S. Puri and A. Aggarwal, Electric Discharge Machining–A Potential Choice for Surface Modification of Metallic Implants for Orthopedic Applications: A Review, *Proc. Inst. Mech. Eng. Part B J. Eng. Manuf.*, 2016, **230**(2), p 331–353
3. K. Yanatori and M. Kunieda, Study on Debris Movement in EDM Gap, *J. Japan Soc. Electr. Mach. Eng.*, 1995, **29**(61), p 19–27. https://doi.org/10.2526/jseme.29.61_19
4. G.S. Prihandana, M. Mahardika, M. Hamdi, Y.S. Wong and K. Mitsui, Accuracy Improvement in Nanographite Powder-Suspended Dielectric Fluid for Micro-Electrical Discharge Machining Processes, *Int. J. Adv. Manuf. Technol.*, 2011, **56**(1–4), p 143–149. https://doi.org/10.1007/s00170-011-3152-6
5. G. Talla, S. Gangopadhyay and C.K. Biswas, Effect of Powder-Suspended Dielectric on the EDM Characteristics of Inconel 625, *J. Mater. Eng. Perform.*, 2016, **25**(2), p 704–717. https://doi.org/10.1007/s11665-015-1835-0
6. S. Sundriyal, J. Yadav and R.S. Walia, Thermophysical-Based Modeling of Material Removal in Powder Mixed Near-Dry Electric Discharge Machining, *J. Mater. Eng. Perform.*, 2020, **29**, p 6550–6569. https://doi.org/10.1007/s11665-020-05110-3
7. X. Wang, C. Li, H. Guo, S. Yi, L. Kong and S. Ding, Alternating Energy Electrical Discharge Machining of Titanium Alloy Using a WC-PCD Electrode, *J. Manuf. Process.*, 2020, **60**, p 37–47. https://doi.org/10.1016/j.jmapro.2020.10.034
8. W.S. Zhao, Q.G. Meng and Z.L. Wang, The Application of Research on Powder Mixed EDM in Rough Machining, *J. Mater. Process. Technol.*, 2002, **129**(1–3), p 30–33. https://doi.org/10.1016/S0924-0136(02)00570-8
9. X. Wang, Y. Liu, Y. Zhang, Q. Sun and Z. Li, Characteristics of Plasma Channel in Powder-Mixed EDM Based on Monopulse Discharge, *Int. J. Adv. Manuf. Technol.*, 2016, **82**, p 1063–1069. https://doi.org/10.1007/s00170-015-7236-6
10. G. Talla, S. Gangopadhayay and C.K. Biswas, State of the Art in Powder-Mixed Electric Discharge Machining: A Review, *Proc. Inst. Mech. Eng. Part B J. Eng. Manuf.*, 2017, **231**(14), p 2511–2526. https://doi.org/10.1177/0954405416634265
11. T. Jadam, S.K. Sahu, S. Datta and M. Masanta, EDM Performance of Inconel 718 Superalloy: Application of Multi-Walled Carbon Nanotube (MWCNT) Added Dielectric Media, *J. Brazil. Soc. Mech. Sci. Eng.*, 2019, **41**(8), p 305. https://doi.org/10.1007/s40430-019-1813-9
12. S. Kumar, R. Singh, A. Batish, T.P. Singh and R. Singh, Investigating Surface Properties of Cryogenically Treated Titanium Alloys in Powder Mixed Electric Discharge Machining, *J. Brazil. Soc. Mech. Sci. Eng.*, 2017, **39**(7), p 2635–2648. https://doi.org/10.1007/s40430-016-0639-y
13. H. Marashi, D.M. Jafarlou, A.A.D. Sarhan and M. Hamdi, State of the Art in Powder Mixed Dielectric for EDM Applications, *Precis. Eng.*, 2016, **46**, p 11–33. https://doi.org/10.1016/j.precisioneng.2016.05.010
14. A. Erden, S. Bilgin, Role of impurities in electric discharge machining, in *Proceedings of 21st International Machine Tool Design and Research Conference*, 1981, pp 345–350. https://doi.org/https://doi.org/10.1007/978-1-349-05861-7_45
15. J.E. Abu Qudeiri, A. Saleh, A. Ziout, A.H.I. Mourad, M.H. Abidi and A. Elkaseer, Advanced electric discharge machining of stainless steels: Assessment of the state of the art, gaps and future prospect, *Materials*, 2019, **12**(6), p 907. https://doi.org/10.3390/ma12060907
16. M. Al-Amin, A.M.A. Rani, A.A.A. Aliyu, M.A.A. Razak, S. Hastuty and M.G. Bryant, Powder Mixed-EDM for Potential Biomedical Applications: A Critical Review, *Mater. Manuf. Processes.*, 2020, **35**(16), p 1789–1811. https://doi.org/10.1080/10426914.2020.1779939
17. T.D. Nguyen, P.H. Nguyen and L.T. Banh, Die Steel Surface Layer Quality Improvement in Titanium M -Powder Mixed Die Sinking Electrical Discharge Machining, *Int. J. Adv. Manuf. Technol.*, 2018, **100**, p 2637–2651. https://doi.org/10.1007/s00170-018-2887-8
18. H. Marashi, A.A.D. Sarhan and M. Hamdi, Employing Ti Nano-Powder Dielectric to Enhance Surface Characteristics in Electrical Discharge Machining of AISI D2 Steel, *Appl. Surf. Sci.*, 2015, **357**, p 892–907. https://doi.org/10.1016/j.apsusc.2015.09.105
19. Y. Chen and Y. Lin, Surface Modifications of Al–Zn–Mg Alloy Using Combined EDM with Ultrasonic Machining and Addition of TiC Particles into the Dielectric, *J. Mater. Process. Technol.*, 2009, **209**, p 4343–4350. https://doi.org/10.1016/j.jmatprotec.2008.11.013
20. S. Tripathy and D.K. Tripathy, Multi-Attribute Optimization of Machining Process Parameters in Powder Mixed Electro-Discharge Machining Using TOPSIS and Grey Relational Analysis, *Eng. Sci. Technol. Int. J.*, 2016, **19**(1), p 62–70. https://doi.org/10.1016/j.jestch.2015.07.010
21. S. Tripathy and D. Tripathy, An Approach for Increasing the Micro-Hardness in Electrical Discharge Machining by Adding Conductive Powder to the Dielectric, *Mater. Today Proc.*, 2017, **4**(2), p 1215–1224. https://doi.org/10.1016/j.matpr.2017.01.140
22. C. Prakash, H.K. Kansal, B.S. Pabla and S. Puri, Experimental Investigations in Powder Mixed Electric Discharge Machining of Ti–35Nb–7Ta–5Zrβ-Titanium Alloy, *Mater. Manuf. Processes.*, 2017, **32**(3), p 274–285. https://doi.org/10.1080/10426914.2016.1198018
23. L. Li, L. Zhao, Z.Y. Li, L. Feng and X. Bai, Surface Characteristics of Ti-6Al-4V by SiC Abrasive-Mixed EDM with Magnetic Stirring, *Mater. Manuf. Processes.*, 2017, **32**(1), p 83–86. https://doi.org/10.1080/10426914.2016.1151043
24. S. Kumar Sahu, T. Jadam, S. Datta, D. Dhupal and G. Nandi, Application of SiC Power Added in Kerosene Dielectric Media for Electro-Discharge Machining of Inconel 718 Super Alloys: Effect of Powder Concentration, *Mater. Today Proc.*, 2018, **5**(9), p 20297–20305. https://doi.org/10.1016/j.matpr.2018.06.402
25. A. Al-Khazraji, S.A. Amin and S.M. Ali, The Effect of SiC Powder Mixing Electrical Discharge Machining on White Layer Thickness, Heat Flux and Fatigue Life of AISI D2 Die Steel, *Eng. Sci. Technol. an Int. J.*, 2016, **19**(3), p 1400–1415. https://doi.org/10.1016/j.jestch.2016.01.014
26. T.T. Öpöz, H. Yaşar, N. Ekmekci and B. Ekmekci, Particle Migration and Surface Modification on Ti6Al4V in SiC Powder Mixed Electrical Discharge Machining, *J. Manuf. Process.*, 2018, **31**, p 744–758. https://doi.org/10.1016/j.jmapro.2018.01.002
27. A.K. Rouniyar and P. Shandilya, Experimental Investigation on Recast Layer and Surface Roughness on Aluminum 6061 Alloy During Magnetic Field Assisted Powder Mixed Electrical Discharge Machining, *J. Mater. Eng. Perform.*, 2020 https://doi.org/10.1007/s11665-020-05244-4
28. F.L. Amorim, V.A. Dalcin, P. Soares and L.A. Mendes, Surface Modification of Tool Steel by Electrical Discharge Machining with Molybdenum Powder Mixed in Dielectric Fluid, *Int. J. Adv. Manuf. Technol.*, 2017, **91**(1–4), p 341–350. https://doi.org/10.1007/s00170-016-9678-x
29. R. Świercz and D. Oniszczuk-świercz, The Effects of Reduced Graphene Oxide Flakes in the Dielectric on Electrical Discharge Machining, *Nanomaterials*, 2019, **9**(3), p 1–16. https://doi.org/10.3390/nano9030335

30. M. Shabgard and B. Khosrozadeh, Investigation of Carbon Nanotube Added Dielectric on the Surface Characteristics and Machining Performance of Ti–6Al–4V Alloy in EDM Process, *J. Manuf. Process.*, 2017, **25**, p 212–219. https://doi.org/10.1016/j.jmapro.2016.11.016
31. M.M. Hossain, M.S.B.A. Karim, W.Y. Hoong, M.H.B.A. Shukor and M.S.B.A. Talip, Feasibility of Using CeO 2 / Water Dielectrical Nanofluid in Electrical Discharge Machining ( EDM ), *Arab. J. Sci. Eng.*, 2020, **45**, p 5435–5445. https://doi.org/10.1007/s13369-020-04404-x
32. G.S. Prihandana, M. Mahardika, M. Hamdi, Y.S. Wong and K. Mitsui, Effect of Micro-Powder Suspension and Ultrasonic Vibration of Dielectric Fluid in Micro-EDM Processes—Taguchi Approach, *Int. J. Mach. Tools Manuf.*, 2009, **49**(12–13), p 1035–1041. https://doi.org/10.1016/j.ijmachtools.2009.06.014
33. B. Jabbaripour, M. Hossein, M. Reza and H. Faraji, Investigating Surface Roughness, Material Removal Rate and Corrosion Resistance in PMEDM of γ-TiAl Intermetallic, *J. Manuf. Process.*, 2013, **15**(1), p 56–68. https://doi.org/10.1016/j.jmapro.2012.09.016
34. S. Kumar and U. Batra, Surface Modification of Die Steel Materials by EDM Method Using Tungsten Powder-Mixed Dielectric, *J. Manuf. Process.*, 2012, **14**(1), p 35–40. https://doi.org/10.1016/j.jmapro.2011.09.002
35. A. Bhattacharya, A. Batish and N. Kumar, Surface Characterization And Material Migration During Surface Modification of Die Steels With Silicon, Graphite And Tungsten Powder in EDM Process, *J. Mech. Sci. Technol.*, 2013, **27**(1), p 133–140. https://doi.org/10.1007/s12206-012-0883-8
36. R. Tyagi, A.K. Das and A. Mandal, Electrical Discharge Coating Using Ws2 and Cu Powder Mixture for Solid Lubrication and Enhanced Tribological Performance, *Tribol. Int.*, 2018, **120**, p 80–92. https://doi.org/10.1016/j.triboint.2017.12.023
37. K.L. Wu, B.H. Yan, F.Y. Huang and S.C. Chen, Improvement of Surface Finish on SKD Steel Using Electro-Discharge Machining with Aluminum and Surfactant Added Dielectric, *Int. J. Mach. Tools Manuf.*, 2005, **45**, p 1195–1201. https://doi.org/10.1016/j.ijmachtools.2004.12.005
38. H.R. Fazli Shahri, R. Mahdavinejad, M. Ashjaee and A. Abdullah, A Comparative Investigation on Temperature Distribution in Electric Discharge Machining Process Through Analytical, Numerical And Experimental Methods, *Int. J. Mach. Tools Manuf.*, 2017, **114**, p 35–53. https://doi.org/10.1016/j.ijmachtools.2016.12.005
39. J. Wang and F. Han, Simulation Model of Debris and Bubble Movement in Consecutive-Pulse Discharge of Electrical Discharge Machining, *Int. J. Mach. Tools Manuf.*, 2014, **77**, p 56–65. https://doi.org/10.1016/j.ijmachtools.2013.10.007
40. Y.S. Wong, L.C. Lim, I. Rahuman and W.M. Tee, Near-Mirror-Finish Phenomenon in EDM Using Powder-Mixed Dielectric, *J. Mater. Process. Technol.*, 1998, **79**(1–3), p 30–40. https://doi.org/10.1016/S0924-0136(97)00450-0
41. Y.F. Luo, The Dependence of Interspace Discharge Transitivity Upon the Gap Debris in Precision Electrodischarge Machining, *J. Mater. Process. Technol.*, 1997, **68**(2), p 121–131. https://doi.org/10.1016/S0924-0136(96)00019-2
42. Y.F. Tzeng and C.Y. Lee, Effects of Powder Characteristics on Electro Discharge Machining Efficiency, *Int. J. Adv. Manuf. Technol.*, 2001, **17**, p 586–592. https://doi.org/10.1007/s001700170142
43. M. Shabgard, S.N.B. Oliaei, M. Seyedzavvar and A. Najadebrahimi, Experimental Investigation and 3D Finite Element Prediction of the White Layer Thickness, Heat Affected Zone, and Surface Roughness in EDM Process, *J. Mech. Sci. Technol.*, 2011, **25**(12), p 3173–3183. https://doi.org/10.1007/s12206-011-0905-y
44. S. Jithin, A. Raut, U.V. Bhandarkar and S.S. Joshi, Finite Element Model for Topography Prediction of Electrical Discharge Textured Surfaces Considering Multi-Discharge Phenomenon, *Int. J. Mech. Sci.*, 2020, **177**, p 105604. https://doi.org/10.1016/j.ijmecsci.2020.105604
45. X. Feng, Y.S. Wong and G.S. Hong, Characterization and Geometric Modeling of Single And Overlapping Craters in Micro-EDM, *Mach. Sci. Technol.*, 2016, **20**(1), p 79–81. https://doi.org/10.1080/10910344.2015.1085317
46. K. Salonitis, A. Stournaras, P. Stavropoulos and G. Chryssolouris, Thermal Modeling of the Material Removal Rate and Surface Roughness for Die-Sinking EDM, *Int. J. Adv. Manuf. Technol.*, 2009, **40**(3–4), p 316–323. https://doi.org/10.1007/s00170-007-1327-y
47. S.N. Joshi and S.S. Pande, Thermo-Physical Modeling of Die-Sinking EDM Process, *J. Manuf. Process.*, 2010, **12**(1), p 45–56. https://doi.org/10.1016/j.jmapro.2010.02.001
48. M. Kolli and A. Kumar, Surfactant and graphite powder-assisted electrical discharge machining of titanium alloy, *Proc. Inst. Mech. Eng. Part B J. Eng. Manuf.*, 2017, **231**(4), p 641–657. https://doi.org/10.1177/0954405415579019
49. V. Prakash, S.P. Kumar, P.K. Singh, A.K. Das, S. Chattopadhyaya, A. Mandal and A.R. Dixit, Surface Alloying of Miniature Components by Micro-Electrical Discharge Process, *Mater. Manuf. Process.*, 2018, **33**(10), p 1051–1061. https://doi.org/10.1080/10426914.2017.1364755
50. H.T. Lee and T.Y. Tai, Relationship Between EDM Parameters and Surface Crack Formation, *J. Mater. Process. Technol.*, 2003, **142**, p 676–683. https://doi.org/10.1016/S0924-0136(03)00688-5
51. D.R. Askelan, P.P. Phule and W.J. Wright, *The Science and Engineering of Materials*, 6th ed. Thomson Brook/Cole, San Francisco, 2010